NTNU – Trondheim
Norwegian University of
Science and Technology

Finite Element Analyses of Spudcan Penetration Using CEL Method

Aleksander Worren

Civil and Environmental Engineering
Submission date: June 2013
Supervisor: Hans Petter Jostad, BAT

Norwegian University of Science and Technology
Department of Civil and Transport Engineering

NORWEGIAN UNIVERSITY OF SCIENCE AND TECHNOLOGY
DEPARTMENT OF CIVIL AND TRANSPORT ENGINEERING

Report Title: Finite element analyses of spudcan penetration using CEL method	Date: 09/06/2013 Number of pages (incl. appendices): 88			
	Master Thesis	X	Project Work	
Name: Aleksander Worren				
Professor in charge/supervisor: Hans Petter Jostad				
Other external professional contacts/supervisors: Steinar Nordal				

Abstract:
A hazard during installation of jack-up spudcans is punch-through, which is characterized by a peak resistance, followed by a significant reduction in spudcan resistance. This might lead to an uncontrolled rapid leg penetration as the installation generally is load-controlled. The problem is typical for sites where a stiff soil layer is overlying a soft clay layer. Accurate calculation of the expected displacement-resistance curve for these soil conditions is therefore important in order to reduce the risk of uncontrolled punch-through conditions.
Numerical simulation of spud-can penetration into seabed during installation of jack-up platforms is a complex problem involving both large strains and large displacements where the geometry changes during penetration e.g. interface between layers. The Coupled-Eulerian-Lagrangion (CEL) method available in the finite element program package ABAQUS is suitable for this type of problem. The main aim of this Master Thesis is therefore to use the CEL method to analyse some published examples of spudcan penetration.
Some preliminary tests were performed in Abaqus/Explicit, namely triaxial, oedometer and T-bar tests. It was revealed that the element size had a large impact on the results, where smaller elements increased the accuracy in general. The compression/penetration rate affected mainly the oscillations that occurred in the results. However, the resistance oscillated around an apparently correct mean value, and it was therefore possible to filter out some of the oscillations.
Two spudcan penetration cases were chosen for calculation. The cases were found in Sindhu Tjahyono's doctor thesis (Tjahyono, 2011). Comparison with Tjahyono's results showed that smaller elements reduce the resistance, while larger elements increase the resistance. This behaviour was also found by the preliminary simulation. The cases with strain-softening were sensitive to mesh size, as the strain-softening were mostly localized in the shear bands, and the thickness to the shear bands were governed by the element size. Consequently can non-conservative result regarding punch-through be obtained if the elements are too small, as the soil behavior becomes more similar to a case where the soil has been fully remolded.
Theoretical hand calculations for spudcan penetration were also investigated. SNAME's guideline proposed in 2002 for two-layered clay was overly conservative. Hossain & Randolph's method calculated the resistance more accurate, and gave a better description of the soil mechanisms, e.g. cavity depth. The method proposed by Tjahyono gave the closest estimate compared to the FEM calculations.
The CEL method in Abaqus/Explicit has proven to be suitable for spudcan penetration problems. The penetration speed affected mainly how much oscillation that occurs in the results. The oscillation may be filtered out as the resistance oscillated around a mean value. The computational cost for these types of problems are large, and it is therefore of interest to find the highest penetration rate for which oscillations may be filtered out. However, there were some difficulties regarding the effects from the element size, especially when trying to include strain-softening behavior. It is important to address this problem, as non-conservative results might be obtained.

Keywords:

1. jack-up rig
2. Spudcan
3. CEL
4. Abaqus/Explicit

NTNU
Faculty of Engineering Science and Technology
Institute of Civil and Transport Engineering

MASTER DEGREE THESIS

Spring 2013
for

Student: Aleksander Worren

Finite element analyses of spud-can penetration using CEL method

BACKGROUND

Numerical simulation of spud-can penetration into seabed during installation of jack-up platforms is a challenging problem involving both large displacements (updated location of the spud-can and geometry changes of soil surface and soil layers) and large strains. In the EU project GeoInstall Dr. Khoa Huynh at NGI has demonstrated that the Coupled-Eulerian-Lagrangion (CEL) method available in the finite element program package ABAQUS is suitable for this type of problem. However, since the method uses an explicit (dynamic) formulation the solution may be sensitive to the loading/penetration rate applied. In addition, since the background mesh is fixed (no adaptive re-meshing) the solution may become very sensitive to the mesh discretisation. Finely, since the deformation/strains during penetration generally locally is extremely large, the strength of the soil may reduce (soften).

TASK

The main aim of this Master Thesis is to use the CEL method to analyse some published examples of spud-can penetration. Special focus should be to consider the effect of loading/penetration rate, mesh density and large strain in clay. A characteristic feature of most marine clays is softening, i.e. a gradual reduction of the undrained shear strength with increasing strain. These analyses are computational time consuming, meaning that the computer resources available at NTNU will limit the work.

Task description

The initial part of the work should include a short literature study of the CEL method. Then, based on this literature review, one should select some suitable examples to be considered in the numerical simulations.

Preferable, in order to obtain experience with the CEL method in the finite element program ABAQUS some idealized laboratory (e.g. oedometer and triaxial tests) and field tests (e.g. T-bar tests) should first be considered. Then the selected spud-can penetration problems should be studied.

The effect of large strain should either directly or indirectly be taken into account. However, the crucial problem of mesh dependency when using a method without any suitable regularisation techniques is not part of this study.

The work should be reported and organized as a technical report with emphasize on presentation and discussion of the obtained results. The results should also be compared with results from conventional bearing capacity equations generally used in the design of this type of foundations.

Professor in charge: Hans Petter Jostad

Other supervisors: Steinar Nordal

Department of Civil and Transport Engineering, NTNU
Date: 07.06.2013

Hans Petter Jostad

Professor in charge (signature)

Preface

This thesis is the finish of my master degreee at the Norwegian University of Science and Technology, NTNU. I would like to thank Dr. Hans Petter Jostad for guidance trouhout this master thesis. I would also like to thank Dr. Khoa Huyan for learning me how to model spudcan penetration using the CEL method in Abaqus/Explicit.

Aleksander Worren

Trondheim, 9. June 2013

Abstract

A hazard during installation of jack-up spudcans is punch-through, which is characterized by a peak resistance, followed by a significant reduction in spudcan resistance. This might lead to an uncontrolled rapid leg penetration as the installation generally is load-controlled. The problem is typical for sites where a stiff soil layer is overlying a soft clay layer. Accurate calculation of the expected displacement-resistance curve for these soil conditions is therefore important in order to reduce the risk of uncontrolled punch-through conditions.

Numerical simulation of spud-can penetration into seabed during installation of jack-up platforms is a complex problem involving both large strains and large displacements where the geometry changes during penetration e.g. interface between layers. The Coupled-Eulerian-Lagrangion (CEL) method available in the finite element program package ABAQUS is suitable for this type of problem. The main aim of this Master Thesis is therefore to use the CEL method to analyse some published examples of spudcan penetration.

Some preliminary tests were performed in Abaqus/Explicit, namely triaxial, oedometer and T-bar tests. It was revealed that the element size had a large impact on the results, where smaller elements increased the accuracy in general. The compression/penetration rate affected mainly the oscillations that occurred in the results. However, the resistance oscillated around an apparently correct mean value, and it was therefore possible to filter out some of the oscillations.

Two spudcan penetration cases were chosen for calculation. The cases were found in Sindhu Tjahyono's doctor thesis (Tjahyono, 2011). Comparison with Tjahyono's results showed that smaller elements reduce the resistance, while larger elements increase the resistance. This behaviour was also found by the preliminary simulation. The cases with strain-softening were sensitive to mesh size, as the strain-softening were mostly localized in the shear bands, and the thickness to the shear bands were governed by the element size. Consequently can non-conservative result regarding punch-through be obtained if the elements are too small, as the soil behavior becomes more similar to a case where the soil has been fully remolded.

Theoretical hand calculations for spudcan penetration were also investigated. SNAME's guideline proposed in 2002 for two-layered clay was overly conservative. Hossain & Randolph's method calculated the resistance more accurate, and gave a better description of the soil mechanisms, e.g. cavity depth. The method proposed by Tjahyono gave the closest estimate compared to the FEM calculations.

The CEL method in Abaqus/Explicit has proven to be suitable for spudcan penetration problems. The penetration speed affected mainly how much oscillation that occurs in the results. The oscillation may be filtered out as the resistance oscillated around a mean value. The computational cost for these types of problems are large, and it is therefore of interest to find the highest penetration rate for which oscillations may be filtered out. However, there were some difficulties regarding the effects from the element size, especially when trying to include strain-softening behavior. It is important to address this problem, as non-conservative results might be obtained.

Sammendrag

En fare ved installasjon av "jack-up" spudcaner er "punch-through", som er karakterisert ved en maks motstand, etterfulgt av en signifikant reduksjon i spudcan motstand. Dette kan føre til en ukontrollert hurtig penetrasjon av jack-up benet siden penetreringen er hovedsaklig last-styrt. Problemet er typisk for områder hvor en stiv jordsjikt ligger over et svakt leirelag. Nøyaktig beregning av den forventede forskyvning-motstand kurven for disse grunnforholdene er derfor viktig for å redusere risikoen for ukontrollerbar "punch-through" forhold.

Numerisk simulering av spud-can penetrering i havbunnen under installasjon av jack-up-plattformer er et komplekst problem som involverer både store spenninger og store forskyvninger med geometriendringer under penetrasjon f.eks grensesnittet mellom lagene. Den Koblede-Euleriske-Lagrang (CEL) metoden tilgjengelig i element programpakken ABAQUS er egnet for denne typen problemer. Hovedformålet med denne master oppgaven er derfor å bruke CEL metoden for å analysere noen publiserte eksempler på spudcan penetrasjon.

Treakseforsøk, oedometer og T-bar tester ble inledningsvis analyser i Abaqus / Explicit. Disse beregningene viste at elementet størrelse hadde en stor innvirkning på resultatene. Mindre elementer reduserte den numeriske ustabiliteten, noe som generelt økte nøyaktigheten. Komprimering/penetrerings- hastigheten påvirket hovedsaklig svingningene i resultatene. Det var alikevel mulig å filtrere ut mestparten av svingningene, siden mostandsfunksjonen svingte rundt en riktig middelverdi.

To spudcan penentrerings eksempler fra Tjahyono's doktor oppgave ble valgt for FEM analyser. Sammeligning med Tjahyonos resultater viste at mindre elementer vil redusere penetreringsmotstanden, mens større elementer vil øke den. Beregningene som inkluderte "strain-softening" var sensitive for elementstørelsen, siden mesteparten av "strain-softening" oppstod i skjær båndene, og tykkelsen på skjær båndene var styrt av elementstørelsen. Dermed var det mulig å få ukonservative resultater med tanke på "punch-through" hvis for små elementer ble brukt. Beregningene ville da bli mer likt et tilfelle der jordlaget er omrørt på forhåd.

De teoretiske løsningsmetodene var også undersøkt. SNAME framgangsmåte som var foreslått i 2002 for to-lags leire var for konservativ. Hossain & Randolphs metode bergnet motstanden mer nøyaktig, samtidig som den beskrev jordmekanismene relativt nøyakt, f.eks hull dybden. Metoden foreslått avTjahyono var nærmest FEM beregingene.

CEL metden i Abaqus/Explicit har vist seg å være godt egnet for spudcan penetrerings problemer. Pennetreringhastigheten påvirket hovedsaklig hvor mye svingninger som var i test resultatene. Disse svingingene var alikevel mulig å filtrere ut, siden motstanden svingte rundt en middelverdi. Det var noen problemer med tanke på effekter fra elementstørelsen, spesielt for de problemene som inkluderte "strain-softening". Det viktig å studere disse effektene, siden ukonservative resulater kan oppstå.

Table of Contents

List of Tables

List of Figures

Chapter 1. Introduction

1.1 Background

Jack-up rigs are the most common type of mobile platforms. They operate at shallow and up to moderate depths (167 meters (World Fleet of Jack-Up Drilling Rigs, 2012)). These rigs are often used as drilling units, but they can also perform other tasks, such as installation of wind turbines. Jack-up rigs have movable legs, which may be jacked down into the seabed to give stabilization under operation, hence the name jack-up. The legs often stand on spudcan foundations, which are steel conical footings. Spudcans have a maximum diameter of 10 to around 20 meters. The main objective to the spudcan is to distribute the load from the jack-up rig and give stability. The spudcan may be penetrated up to tens of meters into the seabed if the soil is soft. The installation is performed by applying vertical load from the jack-rig and water ballast in the hull. This means that the penetration is load controlled, and the average penetration rate is often around 1m/hour (Tjahyono, 2011).

The legs and jack-up rig may be damaged if the penetration rate becomes too large. It is therefore important to know the soil characterization and expected load-response curve. A typical hazard is punch-through during the installation. It is characterized by a peak resistance during the installation, followed by a fast reduction in spudcan resistance. This might lead to a rapid penetration because the installation is load-controlled. This problem is typical for sites where a stiff soil layer is overlying a soft clay layer. Punch-trough of a jack-up leg will cause the platform to tilt which consequently will give rise to large bending moments. The bending moment may lead to failure in the jack-up legs and connection between the legs and rig. This can endanger personnel and result in huge economic loss.

Several studies have been performed on spudcan-penetration with the purpose of finding a good way to calculate the resistance against the penetration depth. Society of naval architects and marine engineers (SNAME) gave in 2002 a guideline for calculating spudcan resistance during penetration of two layered clay. This method is fairly simple and based on Brown & Meyerhof's bearing capacity equations. It uses a whished-in-place approach of a circular footing, which means that geometric changes in the interface between the layers are neglected. The resistance is consequently underestimated for most cases, while the punch-through potential is overestimated. The SNAME approach is therefore a conservative calculation of the spudcan resistance. However, it is only valid for calculating the resistance in the upper layer, and gives little indication of the soil mechanisms at place during the penetration (e.g. back-flow). Hossain & Randolph's method is a more accurate approach which is based on numerical data from centrifuge tests. The resistance is calculated in several stages, because the deformation mechanism changes. The first stage is up to the peak resistance (punch-through depth). The second stage is up to the point where the resistance is given by the lower layer alone. Backflow often starts during this stage, which means that the effective weight of the backflowing soil has to be subtracted from the resistance function. The

resistance is given by only the lower layer in the last stage, and Hossain and Randolph's method for single-layer clay is used at this point. This method is significantly more complicated to calculate, but it describes the soil mechanisms (e.g. backflow depth) more accurate and gives rise to a less conservative estimate of the resistance and punch-through danger. Sindhu Tjahyono showed in his doctor thesis, "Experimental and numerical modelling of spudcan penetration in stiff clay overlying soft clay", that using the CEL method in Abaqus/Explicit can give fairly accurate results for the spudcan resistance. Tjahyono also came up with a method to calculate the resistance which was easier compared to Hossain & Randolph's method. This method requires reading out values from charts regarding the bearing capacity factors.

1.2 Object of this study

The main aim of this master thesis is to use the CEL method in Abaqus/Explicit to analyze some published examples of spudcan-penetration. Special focus will be to consider the effect of large strain in clay, e.g. gradual reduction of the undrained shear strength with increasing strain.

The initial part of the work includes a short literature study of the CEL method, and the hand calculation methods that are developed for spudcan-penetration in two-layered clay.

First, some simpler tests are calculated in order to get familiar with the CEL method in Abaqus/Explicit, namely a triaxial compression test, an oedometer test, and a T-bar penetration test. These tests are relatively simple to model and have theoretical solutions. This is done in order to address problems and limitations of the method before starting with the more complex spudcan-penetration.

Then some published examples of spudcan-penetration in two-layered clay where selected to calculate in Abaqus/Explicit. The problems were found in Sindhu Tjahyono's doctor thesis: "Experimental and numerical modelling of spudcan penetration in stiff clay overlying soft clay". These problems included a simple strain-softening model that where suitable to implement in the material model for the soil.

Chapter 2. Theory

2.1 Abaqus/Explicit

2.1.1 Explicit dynamic analysis

All of the finite element calculations will be executed in Abaqus/Explicit. The dynamic explicit analysis method is explained in detail in the theory manual for Abaqus (Abaqus 6.12 Theory Manual). Only a short summary is given here.

The equations of motion are integrated using the explicit central difference integration rule.

$$\dot{u}^{\left(i+\frac{1}{2}\right)} = \dot{u}^{\left(i-\frac{1}{2}\right)} + \frac{\Delta t^{(i+1)} + \Delta t^{(i)}}{2}\ddot{u}^{(\mathrm{i})}$$
$$u^{(i+1)} = u^{(i)} + \Delta t^{(i+1)} * \dot{u}^{\left(i+\frac{1}{2}\right)}$$

Where u is the displacement, $\dot{u}$ is the velocity and $\ddot{u}$ is the acceleration. The initial increment (i=0) requires one extra calculation as $\dot{u}^{\left(-\frac{1}{2}\right)}$ is not known.

$$\dot{u}^{\left(-\frac{1}{2}\right)} = \dot{u}^{(0)} - \frac{\Delta t^{(0)}}{2}\ddot{u}^{(0)}$$

Lumped element mass matrixes are used. Lumped mass matrixes are diagonal which makes the explicit dynamic procedure very computational efficient because no iterations are required. The acceleration is calculated at the beginning of each increment using the following equation.

$$\ddot{u} = M^{-1} \cdot \left(F^{(i)} - I^{(i)}\right)$$

M is the lumped mass matrix, F the applied load vector, and I the internal force vector. A calculation of a stable time increment is needed since the central difference method is only conditional stable. The stable time increment is the highest eigenvalue in the system.

$$\Delta t \leq \frac{2}{\omega_{max}}\left(\sqrt{1+\xi^2} - \xi\right)$$

Some damping is introduced in Abaqus/Explicit in order to control high frequency oscillations. Damping will reduce the stable time increment. Initially Abaqus/Explicit calculates a conservative maximum frequency by calculating the eigenvalue for each element, rather than calculating the eigenvalue of the whole model.

$$\Delta t = \frac{2}{\omega_{max}^{element}} = \min\left(\frac{L_e}{c_d}\right)$$

L_e is the characteristic length of the smallest element in the model, and c_d is the dilatation wave speed in the material. Abaqus/Explicit also contains a global estimation algorithm that calculates the maximum frequency for the entire model, which is used as the step proceeds.

2.1.2 Coupled Eulerian-Lagrangian (CEL)

Lagrangian elements have material fixed to the nodes. As a result, the elements will deform as the material deforms. This may lead to numerical problems in large deformation problems. Heavily distorted elements will not work well, and problems like mesh locking, and numerical instability can follow.

In eulerian element formulation, the nodes are fixed in space (coordinate system), while the material is free to move (flow) through the mesh (Abaqus 6.12 Analysis User's Manual). The mesh will consequently not deform as the material deforms. Figure 2-1 shows the deformation of a lagrangian mesh over the deformation of a eulerian mesh. This is particularly useful when dealing with large deformation, where the lagrangian elements would get heavily distorted and encounter numerical problems.

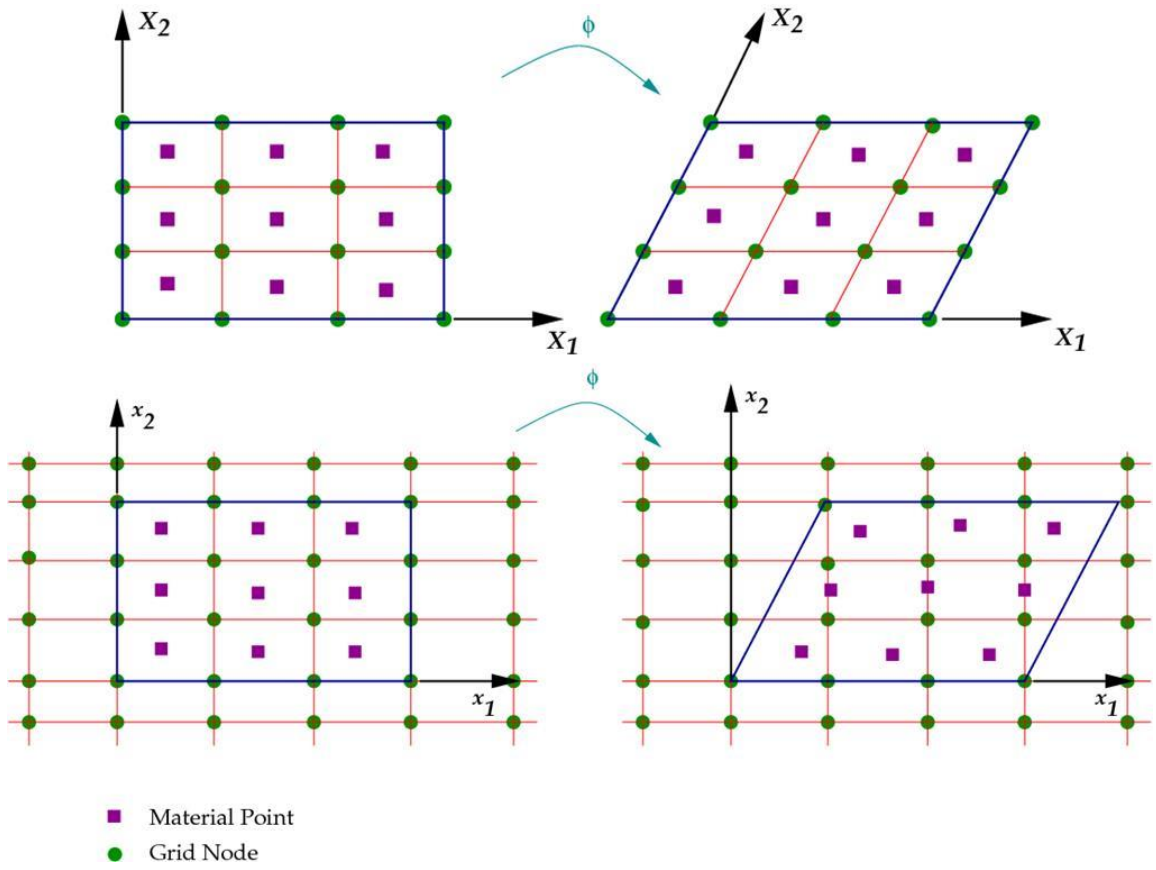

Figure 2-1 Lagrangian element deformation on the top, and eulerian deformation at the bottom. (Nonlinear finite elements/Lagrangian and Eulerian descriptions, 2010)

It is possible to have more than one material in the eulerian mesh using Abaqus/Explicit. The materials are assigned using initial conditions in the start of the analysis. The elements are by default empty (volume fraction = 0), while the volume fraction is one when the element is completely filled with material (Figure 2-2). The material is tracked as it moves through the mesh by calculating the eulerian volume fraction (EVF) of each element. The eulerian material will disappear from the simulation if it moves outside the mesh. The material boundaries (interfaces) are tracked using the computed eulerian volume fraction by each incrementation. Abaqus/Explicit uses an interface reconstruction algorithm that approximates a planar boundary within each element (Abaqus 6.12 Analysis User's Manual). The simplification with planar boundary may lead to discontinues in the interfaces if a coarse mesh is used.

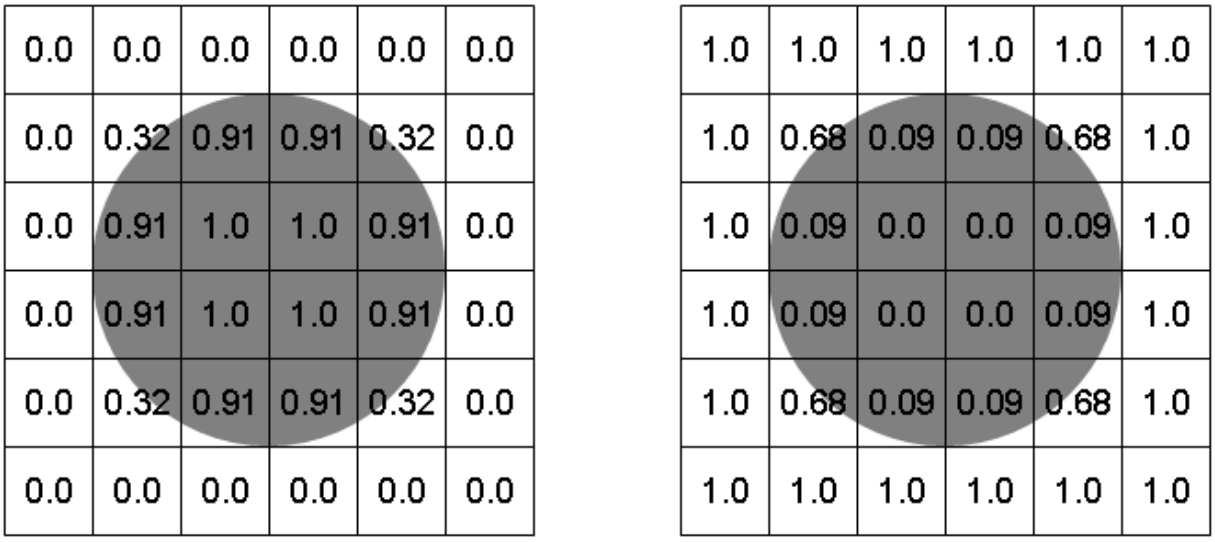

Figure 2-2 Volume fractions (Abaqus/CAE User's Manual)

The deformation of the eulerian material is calculated using an operator split of the governing equations (Abaqus 6.12 Analysis User's Manual). First the Lagrangian phase is calculated, then an Eulerian phase (transport phase), this is also called "Lagrange-plus-remap" formulation. During the Lagrangian step, the eulerian mesh is allowed to deform and follow the material. Next step is that this solution is mapped back to the undeformed eulerian mesh, and the material flow within the neighboring elements is calculated.

2.2 Triaxial compression test

Triaxial compression tests are preformed to establish material parameters for a soil sample, such as friction angle and cohesion. The test is executed with constant confining pressure ($\Delta\sigma_2' = \Delta\sigma_3' = 0$), while the sample is loaded vertically. The vertical displacement and volume changes are measured. The test is preformed drained or undrained.

From Hooke's law, and constant confining pressure, we get the following relations (Nordal, 2012).

$$\Delta\varepsilon_1 = \frac{1}{E}(\Delta\sigma_1' - \nu\Delta\sigma_2' - \nu\Delta\sigma_3')$$

$$\Delta\varepsilon_2 = \frac{1}{E}(\Delta\sigma_2' - \nu\Delta\sigma_1' - \nu\Delta\sigma_3')$$

$$\Delta\varepsilon_3 = \frac{1}{E}(\Delta\sigma_3' - \nu\Delta\sigma_1' - \nu\Delta\sigma_2')$$

$$\Delta\sigma_2' = \Delta\sigma_3' = 0$$

$$\Delta\varepsilon_1 = \frac{1}{E}\Delta\sigma_1'$$

The maximum stress in the sample is two times the size of the undrained shear strength ($\sigma_{1,max}' = 2c_u$) assumed pure cohesive soil and zero confining pressure ($\sigma_2' = \sigma_3' = 0$). The maximum stress may also change after yielding occurs if strain-softening is included. Then the cohesive yield stress is a function of the plastic strain (ε_p). The plastic strain is defined in the Abaqus user manual (Abaqus/CAE User's Manual).

$$\varepsilon_p = \sqrt{\frac{2}{3}}\left[\left(\varepsilon_x^p\right)^2 + \left(\varepsilon_y^p\right)^2 + \left(\varepsilon_z^p\right)^2 + 2\left\langle\left(\varepsilon_{xy}^p\right)^2 + \left(\varepsilon_{xz}^p\right)^2 + \left(\varepsilon_{yz}^p\right)^2\right\rangle\right]^{\frac{1}{2}}$$

For the triaxial test where $\varepsilon_x^p = \varepsilon_y^p = -\nu\varepsilon_z^p$, then ε_p is reduce to:

$$\varepsilon_p = \varepsilon_z * \sqrt{\frac{2}{3}[1 + 2\nu^2]}$$

The triaxial compression test can be used to study the performance of the material model in the finite element model.

2.3 Oedometer test

Oedometer test simulates one dimensional deformation in plane strain ($\varepsilon_2 = \varepsilon_3 = 0 \cup \Delta\sigma_2' = \Delta\sigma_3'$). The sample is constrained in the horizontal direction and loaded vertically. The test is performed under drained conditions ($\nu < 0.5$), where the water is allowed to flow vertically out of the sample. It is a useful test for determine the consolidation properties.

The following relation is valid before yielding occurs in the sample (Nordal, 2012).

$$\Delta\sigma_1' = \frac{E(1-\nu)}{(1-2\nu)(1+\nu)}\Delta\varepsilon_1 = E_{oed}\Delta\varepsilon_1$$

The true stress-strain relation is used for large deformation (Cook, R.D. & Malkus, D.S. & Plesha, M.E. & Witt, R.J, 2002), since the tension shall go to infinite for full compression ($\lim_{\Delta h \to h} \sigma_1 = \infty$).

$$\varepsilon = \ln\left(1 - \frac{\Delta h}{h}\right)$$

This test will be modeled in Abaqus/Explicit to study how the eulerian elements preform under high compression.

2.4 T-bar penetration

The T-bar penetration test is similar to the CPT (Cone Penetration Test) except that it is a horizontal cylinder that is pushed through the soil. It is used to define the cohesion for soft clays. The resistance is measured during the penetration, and the undrained resistance force is calculated.

$$\frac{P}{s_u d} = N_b$$

P is the force per unit length acting on the cylinder, s_u is the undrained shear strength, *d* is the diameter of the cylinder, and N_b is the bar factor. The bar factor is dependent on the roughness of the cylinder. The theoretical value is approximately 12 for rough contact, and 9 for smooth contact (Randolph, M.F. & Houlsby, G.T., 1984) (Stewart, D.P. & Randolph, M.F., 1994). This factor is theoretical, and is based on a plastic solution with a soil model which is elastic-perfectly plastic. Effects like strain-rate dependency, strain-softening and anisotropy are not included. Strain-rate dependency and strain-softening is shown to have a significant effect on the bar factor (Liyanapathirana, 2008), while the bar factor is relatively insensitive to anisotropy (Randolph, M.F. & Andersen, K.H., 2006).

2.5 Spudcan resistance

I will use three different approaches for calculating the spudcan resistance: SNAME, Hossain and Randolph's method, and the method proposed by Sindhu Tjahyono.

2.5.1 Brown & Meyerhof

The bearing capacity for a circular footing on two layer clay is given by equation (Tjahyono, 2011):

$$q_f = 3.0\frac{H}{B}c_{u1} + 6.05c_{u2}$$

H is the thickness of the upper layer, B is the diameter of the footing. c_{u1} and c_{u2} is the cohesive yield strength of namely the upper and lower layer.

2.5.2 SNAME

Society of naval architects and marine engineers (SNAME) gave in 2002 a guideline for calculating spudcan resistance during penetration of two layered clay. This method is fairly simple and based on Brown & Meyerhof's bearing capacity equation. It is widely used in practice for calculating the spudcan resistance, but it has some weaknesses which I will get into. The theory was found in (Tjahyono, 2011).

The bearing load Q, is calculated using the two equations:

For no backflow:

$$Q = A\left[3\frac{h}{B}c_{u1} + N_c s_c\left(1 + 0.2\frac{D+h}{B}\right)c_{u2} + p_0'\right] \leq A(N_c s_c d_c c_{u1} + p_0')$$

Full backflow:

$$Q = A\left[3\frac{h}{B}c_{u1} + N_c s_c\left(1 + 0.2\frac{D+h}{B}\right)c_{u2}\right] + \gamma' V \leq AN_c s_c d_c c_{u1} + \gamma' V$$

A is the maximum horizontal cross section of the spudcan, where *B* is the equivalent diameter. *H* is the thickness of the upper layer, and *D* is the penetration depth, while *h = H - D*. c_{u1} is the cohesion of the upper layer, and c_{u2} the lower layer. N_c is the bearing capacity of factor of a strip footing (5.14 for a circular spudcan), and s_c is the bearing capacity shape factor. p_0' is the effective overburden pressure on side of the spudcan at depth *D*, and d_c bearing capacity depth factor. $\gamma' V$ is the effective soil weight of the soil which is replaced by the spudcan.

This solution uses a wished-in-place approach, which means that the bearing capacity is calculated at various depths to get the load-response during a spudcan penetration (Figure

2-3). The main drawback with this approach is that it does not account for the deformations during the penetration. The interface between the layers will change during the penetration, as some of the upper layer will be pushed into the lower layer. This mechanism tend to increase the spudcan resistance (if $c_{u1}>c_{u2}$), which means that the SNAME approach often lead to underestimated resistance, and overestimated potential for punch-through (Tjahyono, 2011). However, the result will be conservative, but the approach will only give the resistance in the upper layer ($D \leq H$).

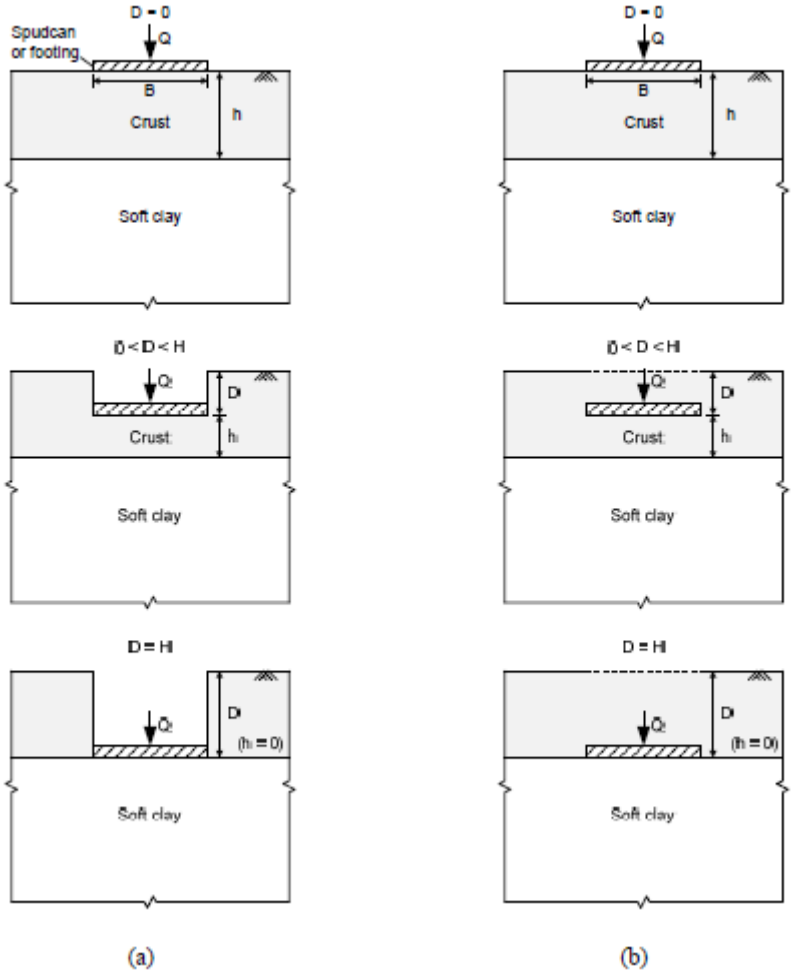

Figure 2-3 Soil geometry during penetration in SNAME: (a) no backflow and (b) full backflow Picture retrieved from (Tjahyono, 2011)

2.5.3 Hossain & Randolph's method

Hossain and Randolph developed a set of equations to calculate load-displacement more accurately during spudcan penetration. The equations are based on curve-fitting data from a series of spudcan penetration tests in two layered clay, which makes this approach more complicated. The response is calculated in stages (Figure 2-4). Stage 1 is the depth where the peak strength occurs (or the depth where punch-through starts). Stage 2 is the depth where only the lower layer gives resistance. The theory was found in (Tjahyono, 2011) and (Hossain, 2008).

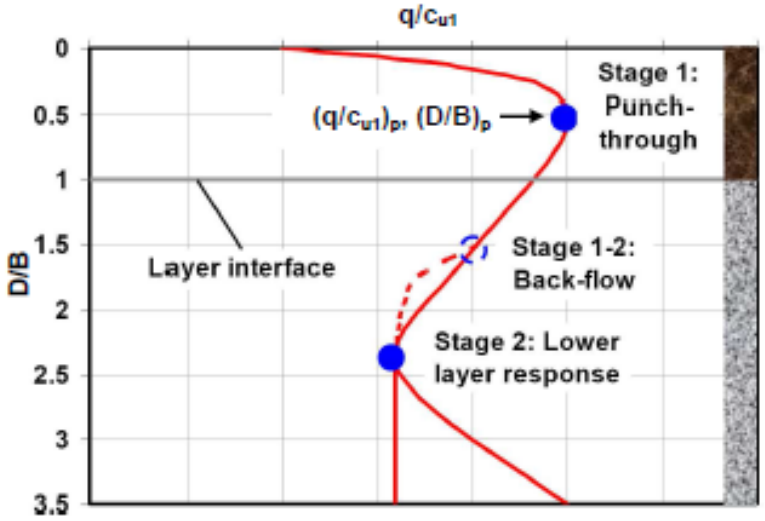

Figure 2-4 Stages in Hossain & Randolph's method. (Tjahyono, 2011)

The response up to step 1 is calculated by the following set of equations:

$$\left(\frac{q}{c_{u1}}\right)_p = 2.9\ln\left[\left(\frac{c_{u2,0}}{c_{u1}}\right)\left(\frac{H}{B}\right)\left(1+\frac{kD}{c_{u2,0}}\right)\right] + 9.9 \le 12$$

$$\left(\frac{D}{B}\right)_p = 1.3\left[\left(\frac{c_{u2,0}}{c_{u1}}\right)\left(\frac{H}{B}\right)\left(1+\frac{kD}{c_{u2,0}}\right)\right]^{1.3}$$

$$\left(\frac{q}{c_{u1}}\right) / \left(\frac{q}{c_{u1}}\right)_p = 0.12\ln\left[\left(\frac{D}{B}\right) / \left(\frac{D}{B}\right)_p\right] + 1$$

$c_{u2,0}$ is the strength at the top of the lower layer, while k is the inclination of strength versus depth. $\left(\frac{D}{B}\right)_p$ gives the depth where the peak strength occurs, normalised by the spudcan diameter B.

The response between stage 1 and 2 is based on failure mechanism shown in Figure 2-5.

$$q = \frac{4(H_{plug,t}c_{u1} + H_{plug,b}c_{u,avg})}{B} + N_{c,deep}c_{u2}^{*} + \gamma_1' H + \gamma_2' H_{plug,b} - \gamma_1' H_{plug}$$

c_{u2}^{*} is the strength at the depth of $H_{plug} + D$ (Figure 2-5). $c_{u,avg}$ is the average of the upper and lower clay strengths. H_{plug} is the thickness of the soil "trapped" beneath the spudcan.

While $H_{plug,t}$ is the thickness of the plug which is in the upper layer, and $H_{plug,b}$ the lower layer.

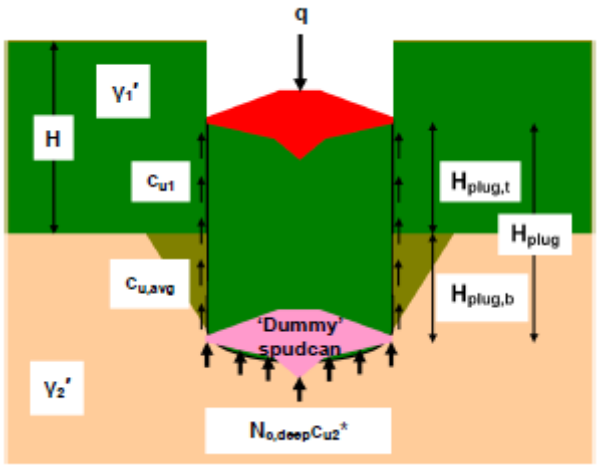

Figure 2-5 Failure mechanism between stage 1 and 2 in Hossain and Randoplh (2009a)'s method. Picture retrieved from (Tjahyono, 2011)

$$\frac{H_{plug}}{H} = f_1 \exp\left(-f_2 \frac{D}{B}\right) \leq 1$$

$$f_1 = 0.17\left(\frac{c_{u2,0}}{c_{u1}}\right)\left(1 + 3.3\frac{kD}{c_{u2,0}}\right) + 1$$

$$f_2 = \left(\frac{c_{u2,0}}{c_{u1}}\right)\left(1 + 1.9\frac{kD}{c_{u2,0}}\right) + 0.25$$

$$N_{c,deep} = N_{c,limit}\left[1 - \exp\left(-\min\left(10{,}2\left(\frac{H_{plug,b}}{B}\right)^{0.5}\right)\right)\right]$$

Where $N_{c,limit} = 13$. The depth of initiated backflow is equivalent to the limiting cavity depth. This is the depth for which the spudcan will be covered in soil, and it is calculated using equations:

$$\frac{d_s}{B} = \left(\frac{c_{u1}}{\gamma_1' B}\right)^{0.55}, \qquad for\ d_s \leq H$$

$$\frac{d_s}{B} = 1.4\left[\left(\frac{c_{u1}}{\gamma_2' B}\right)\left(\frac{H}{B}\right) / \left(1 + \frac{kB}{c_{u2,0}}\right)\right]^{0.5}, \qquad for\ d_s > H$$

The effective weight of the soil which flow on top of the spudcan has to be subtracted from the resistance equation.

Stage 2 is at the depth where the response is affected by only the lower layer. It is found at the intersection point between the response from the previous equations, and the response given by Hossain and Randolph's method for single layer clay (Tjahyono, 2011). The response is then given by the single layer clay approach for the lower layer (Hossain, M.S. & Randolph, M.F., 2009) after stage 2.

If the clay has uniform strength with depth:

$$q = N_{c0}c_{u2} + \gamma_2' D + \gamma_2' \frac{V_b}{A}, \qquad for\ D \le d_s$$

$$q = N_{cd}c_{u2} + \gamma_2' \frac{V_b}{A}, \qquad for\ D > d_s$$

$$N_{cd} = 12.9\left[max\left(0.05, \left(\frac{D-d_s}{B}\right)\right)\right]^{0.11} \le 12 \qquad Smooth\ base$$

$$N_{cd} = 13.6\left[max\left(0.05, \left(\frac{D-d_s}{B}\right)\right)\right]^{0.11} \le 13.1 \qquad Rough\ base$$

Where V_b is the volume of the embedded spudcan below the maximum diameter.

If the clay has increasing strength with depth:

$$q = N_{c0k}c_{u2} + \gamma_2' D + \gamma_2' \frac{V_b}{A}, \qquad for\ D \le d_s$$

$$q = N_{cdk}c_{u2} + \gamma_2' \frac{V_b}{A}, \qquad for\ D > d_s$$

$$N_{c0k} = N_{c0}\left[1 + 0.161\left(\frac{kB}{c_{u2,D}}\right)^{0.8} / \left(1 + \frac{D}{B}\right)^2\right]$$

$$N_{cdk} \approx 10\left(1 + 0.065\frac{D}{B}\right) \le 11.3$$

This method is clearly more complicated than SNAME, and requires a lot more calculation. But it has several advantages. It is based on numerical data, and is not subject to the problems with the whished-in-place approach. It may also account for increasing strength with depth in the lower layer clay. However, it will not work properly for low values of H/B (thin crust). It may give zero or negative spudcan resistance in stage 1 (Tjahyono, 2011).

2.5.4 Sindhu Tjahyono's method

The theory for this approach is found in Tjahyono's doctor thesis (Tjahyono, 2011). The limiting cavity is given similar to as in Hossain & Randolph's method. If the cavity depth is within the upper layer:

$$\frac{d_s}{B} = \left(\frac{c_{u1}}{\gamma_1' B}\right)^{0.55}, \qquad for\ \frac{H}{B} \geq \left(\frac{c_{u1}}{\gamma_1' B}\right)^{0.55}$$

And if the cavity depth is in the lower layer:

$$\frac{d_s}{B} = \left(\frac{c_{u2}}{\gamma_2' B}\right)^{0.55} \geq \frac{H}{B} + 0.4\left(1 - \frac{c_{u2}}{c_{u1}}\right), \qquad for\ \frac{H}{B} < \left(\frac{c_{u1}}{\gamma_1' B}\right)^{0.55}$$

The spudcan resistance in weightless soil is given by the following equation (back-flow does not occur in weightless soil).

$$q_0 = c_{u1} N_c^*$$

The N_c^* factor is given in figures in Tjahyono's doctor thesis "Experimental and numerical modeling of spudcan penetration in stiff clay overlying soft clay". The factor depends on the thickness of the upper layer, depth of penetration, and strength ratio of the soils.

The spudcan resistance before backflow ($D \leq d_s$), including the soil-weight, is calculated from the following equations.

$$q = c_{u1} N_c^* + \gamma_1' D, \quad if\ D \leq H$$
$$q = c_{u1} N_c^* + \gamma_1' H + \gamma_2'(D - H), \qquad if\ D > H$$

The following set of equations is used when back-flow is initiated.

$$q = c_{u1} N_c^* + \gamma_1' d_s + \frac{\gamma_1' V}{A} \leq c_{u1} N_c^* + \gamma_1' D, \qquad if\ d_s \leq H$$
$$q = c_{u1} N_c^* + \gamma_1' H + \gamma_2'(d_s - H) + \frac{\gamma_1' V}{A} \leq c_{u1} N_c^* + \gamma_1' H + \gamma_2'(D - H), \qquad if\ d_s > H$$

This method seems fairly simple, and the N_c^* factors are given in Tjahhyono's doctor thesis (Tjahyono, 2011). However, the N_c^* factor is only given for $\frac{H}{B} \leq 1$.

2.6 Finite element models

A simple Mohr Coulomb material model is used for all the numerical calculations in Abaqus/Explicit. The parameters which needs to be defined is the elasticity modulus (E), poisons ratio (v), friction angle (zero in all analysis), dilatation angle (zero), and the cohesive yield strength (c) related to the absolute plastic strain (ε_p).

The absolute plastic strain is defined in the theory manual in Abaqus (Abaqus/CAE User's manual).

$$\varepsilon_p = \sqrt{\frac{2}{3}}\left[\left(\varepsilon_x^p\right)^2 + \left(\varepsilon_y^p\right)^2 + \left(\varepsilon_z^p\right)^2 + 2\left\langle\left(\varepsilon_{xy}^p\right)^2 + \left(\varepsilon_{xz}^p\right)^2 + \left(\varepsilon_{yz}^p\right)^2\right\rangle\right]^{\frac{1}{2}}$$

The yield criterion in the model is:

$$\tau = c - \sigma\sin(\phi)$$

The Mohr-Coulomb model is reduced to a pressure independent Tresca model when $\phi = 0°$ (Abaqus/CAE User's Manual).

The structures (spudcan, T-bar and plates) in the calculations are modeled using 8-node lagrangian brick elements with reduced integration (C3D8R). They are completely constrained to a reference point, so they act as rigid elements that follow the movement to the reference point. I have chosen this approach because of the high stiffness in the structures compared to the soil. The small deformations in the structures are not counted for in this approach, which are also not of interest in this study.

The soil is modeled as 8-node linear eulerian brick elements with reduced integration and hourglass control. This is the only element type available in Abaqus/Explicit for the eulerian elements.

The interaction between the soil (eulerian) and structure (lagrangian) elements was modeled using the general contact in Abaqus/Explicit. And the penalty method was used for the tangential behavior with a friction coefficient of 1 for fully rough contact.

Chapter 3. Preliminary calculations

3.1 Triaxial test

A triaxial compression test with zero confining pressure is a simple way to check the performance of the coupled eulerian lagrangian method in Abaqus/Explicit. The objective of the test was to check the post yield behavior and if the elasticity modulus was properly used. Softening was also introduced to see if strain softening behavior was possible to implement in the model.

3.1.1 Mesh convergence

First a mesh convergence test was performed, with no strain-softening behavior. The soil was modeled as a cylinder with diameter of 0.1 meters and a height of 0.2 meters (Figure 3-1). The soil was compressed between two plates. The left picture shows the eulerian mesh, and the two rigid plates, and the picture to the right shows the active eulerian elements (at the beginning of the analysis) between the plates.

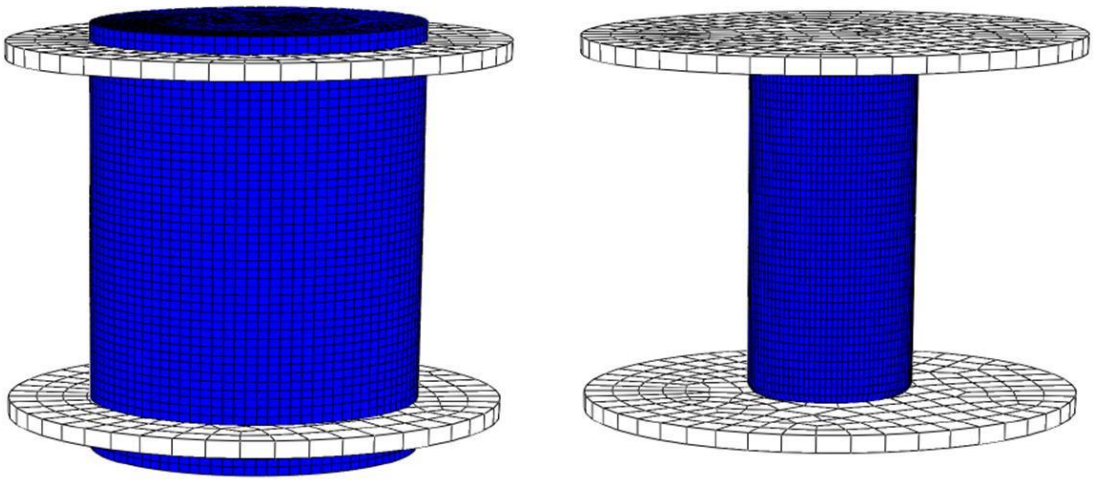

Figure 3-1 Triaxial model

The bottom plate was fixed, while the top plate was given a constant velocity of 0.01 m/s. The interaction between the soil (eulerian) and plate (lagrangian) elements was modeled using the general contact in Abaqus/Explicit. The penalty method was used for the tangential behavior with a friction coefficient of 0.01, which appeared to be low enough to allow sliding, while keeping the plates in contact with the soil (except for the coarsest mesh).

The properties of the soil are listed in the table below.

Young's modulus (E)	1000 kPa
Poisson's ratio (ν)	0.3
Cohesion yield stress (c)	10 kPa
Friction angle (ϕ)	0°
Dilatation angle (ψ)	0°

Table 1 Soil properties for triaxial compression test

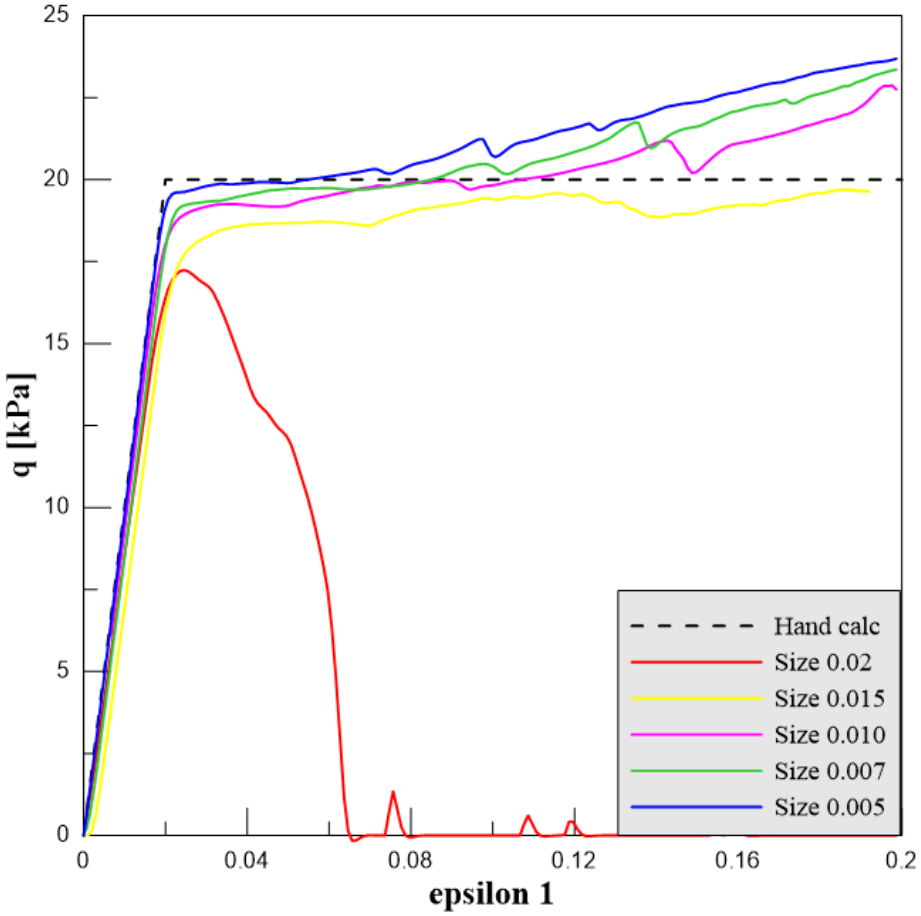

Figure 3-2 Mesh convergence

The model with the coarsest mesh lost contact with the plates during the calculation. Young's modulus is correctly applied, seemingly independent of the mesh size. The yield strength is underestimated for all the models, but converges to the right value for increased mesh resolution. The post yielding behavior shows increased strength in the FEM calculations, and the effect is amplified as the element size decrease. The reason for the deviation from the theoretical solution (hand calculation) is that the deformation mode is non-homogeneous (Figure 3-3). This means that it is different strain and tension in different elements. It is also different geometric changes.

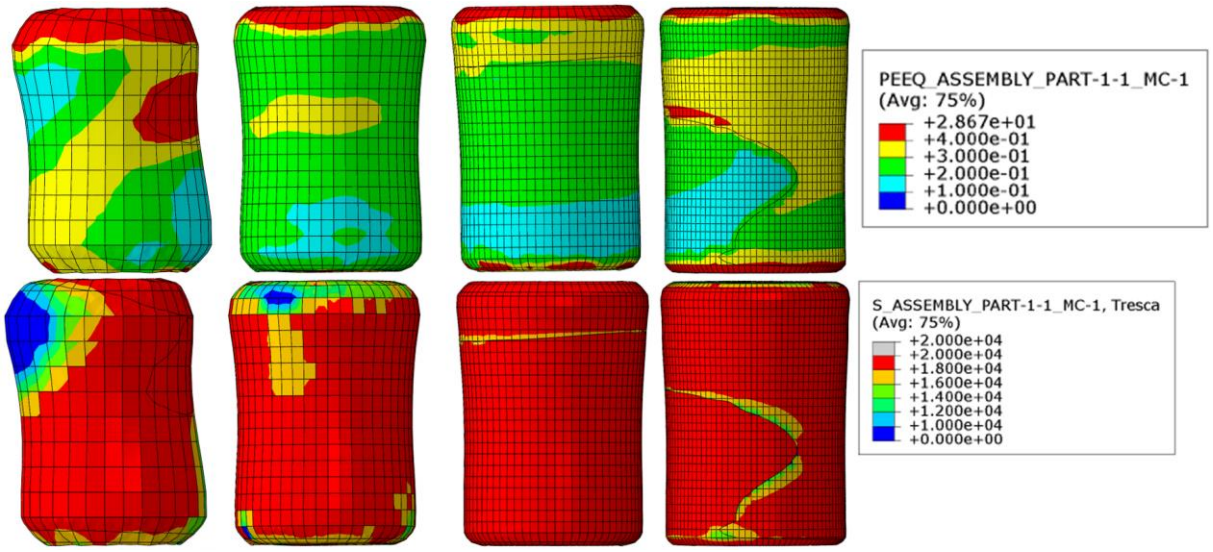

Figure 3-3 Contour plot of Tresca stress & absolute plastic strain for the deformed models

A good way to check the performance of the model is to study the energy balance. The kinetic energy is supposed to be low compared to the internal energy. The artificial energy should also be low, less than 10% of the internal energy (Cook, R.D. & Malkus, D.S. & Plesha, M.E. & Witt, R.J, 2002). High artificial energy indicates that hourglassing and numerical instability may be a problem. Refining the mesh resolution usually reduces the amount of artificial energy.

Element size	0.020	0.015	0.010	0.007	0.005
Internal Energy [Nm]	2.93	6.68	6.56	6.50	6.54
Artificial Energy [Nm]	0.612	0.364	0.169	0.120	0.055
Artificial Energy [%]	20.88%	5.45%	2.58%	1.84%	0.84%
Kinetic Energy [Nm]	2.70E-03	2.96E-04	3.76E-04	7.95E-05	7.56E-05

Table 2 Energy at end of compression in the triaxial test for mesh convergence

It is not a problem with hourglassing and numerical instability in the models, except for the model with the largest element size (which loses contact with the plates). The kinetic energy is also low which is important, as this test is supposed to be quasi-static.

3.1.2 Speed reduction

In an effort to reduce the error, calculations with different speed on the plate was conducted. A model with element size of 0.0035 for the initially active elements, and 0.005 for the empty elements was used.

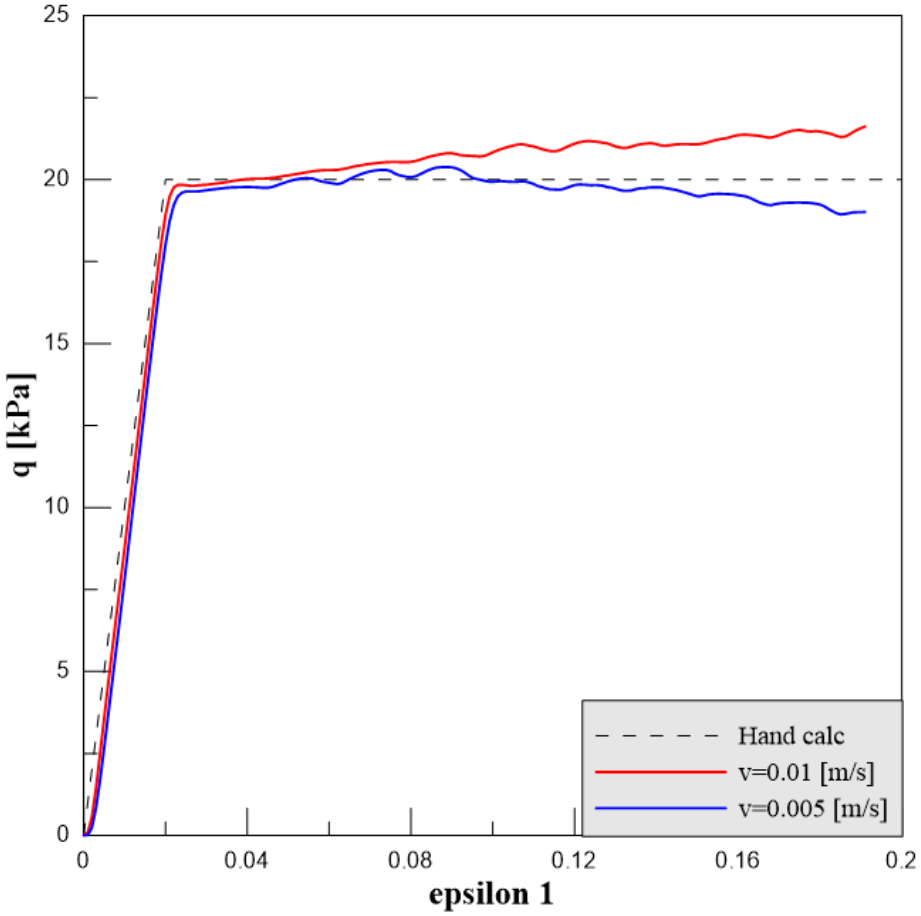

Figure 3-4 Compression speed

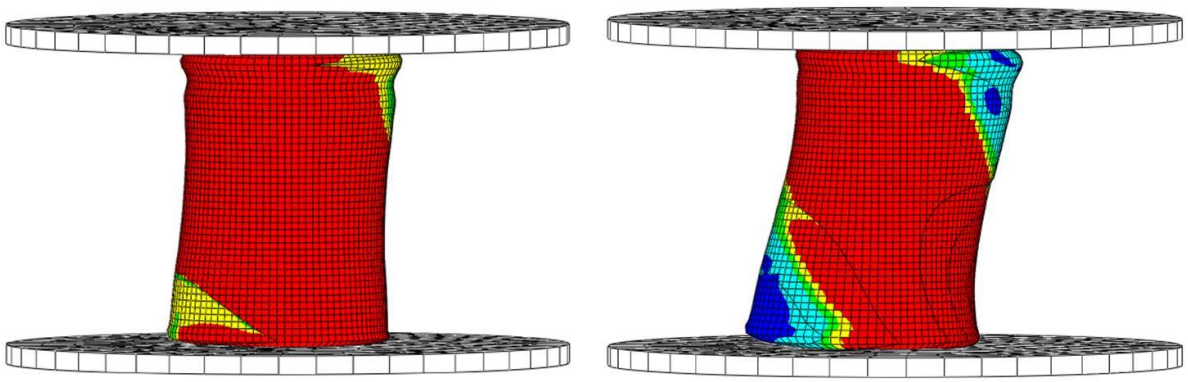

Figure 3-5 Deformed models, subject to different compression speed. Pic from left: V=0.010m/s, V=0.005m/s

The results show that the post yielding response is affected by the speed of the compression. Higher resistance is calculated if the speed is higher, while the resistance may get reduced if the speed is low. However, the reduced resistance for the low-speed analysis is a result of failing soil. As seen in Figure 3-5 of the deformed soil sample, more excessive shear bands are established for the slow analysis (right picture) and the sample appears to slide out of position. The compression speed will therefore change the failure mode. To reduce the possibility of inhomogeneous deformation can more boundary conditions be used, e.g. symmetry planes. The test is in reality quasi-static, so an effort has to be made to keep the speed low. However, reduced speed will naturally increase the calculation time (for same extent of deformation).

3.1.3 Strain-Softening

Strain-softening was then introduced to the calculation. The element size is still 0.0035 for the active elements but 0.010 for the empty elements. An additional calculation was executed on a coarser mesh. This model had element size 0.010 for the active elements, and 0.015 for the initially empty elements. The cohesive yield strength is given for different absolute plastic strain. The sensitivity is set to 2 (A=2), which means that the cohesive yields strength goes from 10 kPa to 5 kPa. The yields strength is kept at 10 kPa until the absolute plastic strain is 0.02, then it is then reduced linearly to 5 kPa at 0.04 plastic strain and kept constant at this value (μ =0.04). The absolute plastic strain is function of the vertical strain, and Poisson's ratio.

$$\varepsilon_p = \varepsilon_z * \sqrt{\frac{2}{3}[1 + 2\nu^2]}$$

Yielding is established as $\sigma_z = 20kPa$ and $\varepsilon_z = 0.02$. The yield strength is then constant until $\varepsilon_z \approx 0.0425$, and reduced to half the strength at $\varepsilon_z \approx 0.0651$.

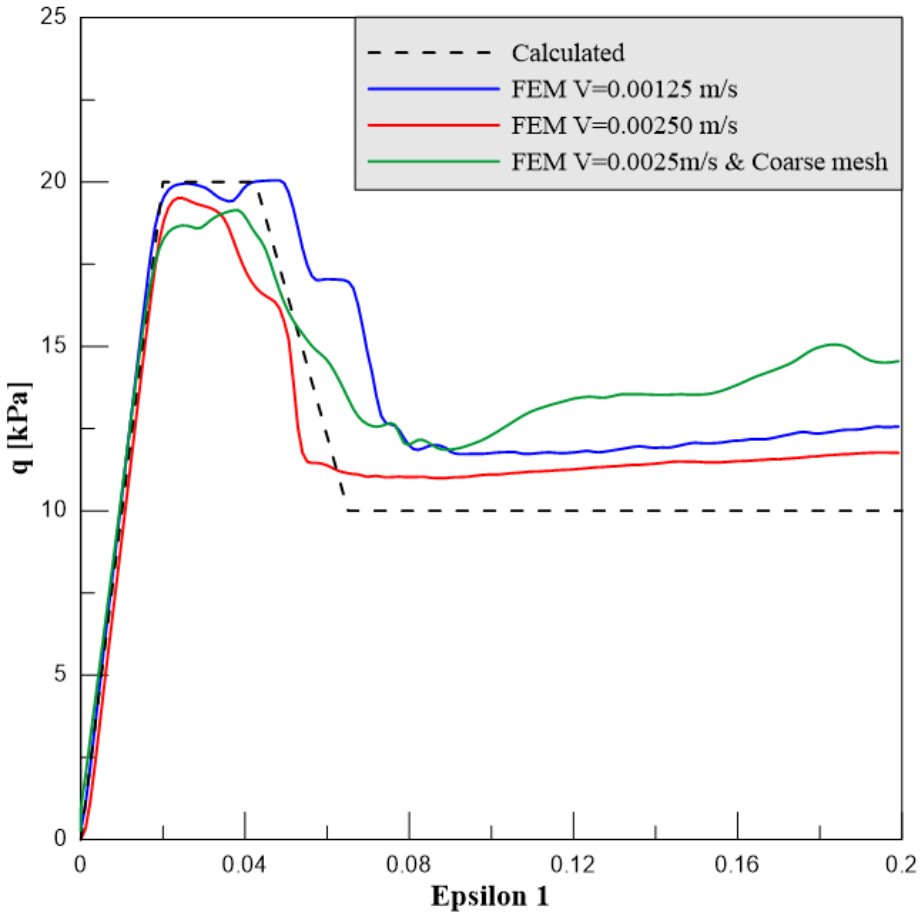

Figure 3-6 Triaxial compression with strain softening

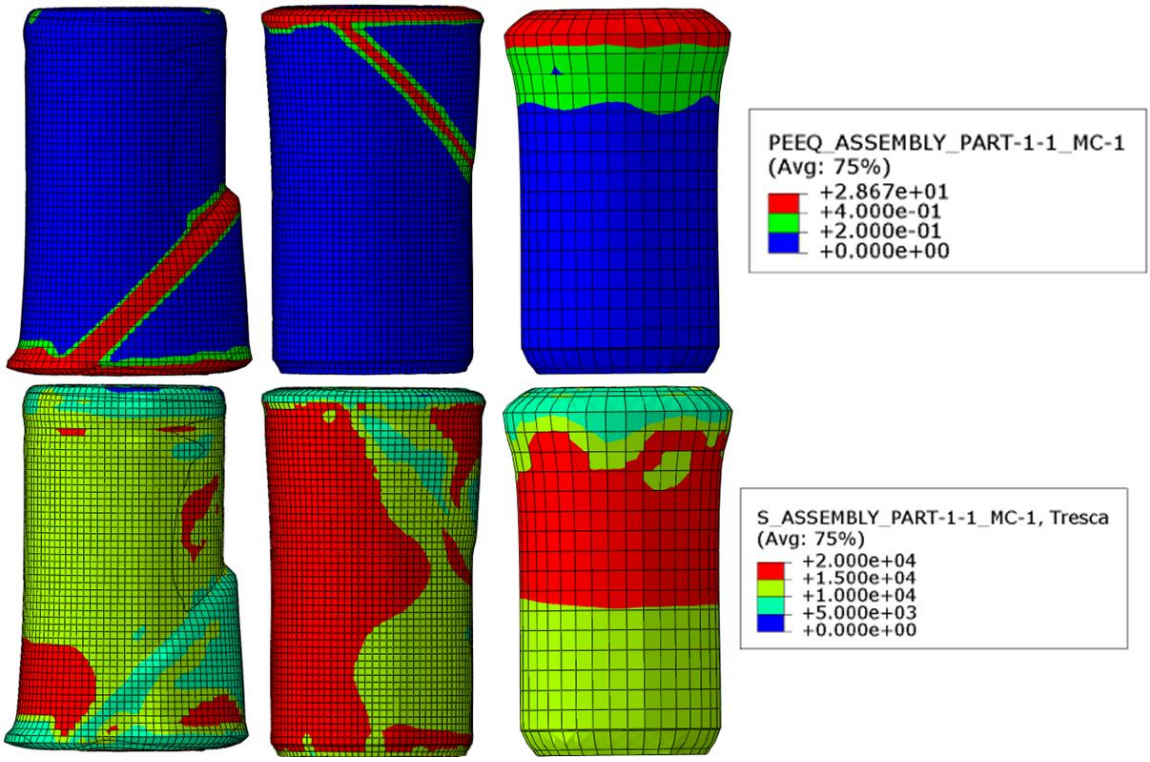

Figure 3-7 Absolute plastic strain and Tresca contour plots at failure ($\varepsilon_1 \approx 0.07$). Pic from left: V=0.0025m/s, V=0.0125m/s, Coarse mesh.

The calculations show that strain-softening can be hard to calculate. The main reason for the deviance from the theoretical solution is because some of the soil has not softened, which is a result of the deformation being localized in the shear bands that are established (Figure 3-7). However, this does not mean that the solutions are wrong, because the theoretical solution is based on homogenous deformation, while the FEM analysis gives a non-homogenous deformation that is more typical for soils. This can be seen in Figure 3-7 of the deformed soil samples with colored Tresca stress. The FEM model with the slowest compression produced a higher resistance and more accurate yield strength. This was not expected, as slower compression speed reduced the resistance for the non-softening material. The slow compression will lead to less softening behavior in the sample, as seen in Figure 3-7. This indicates that the speed of the compression mainly affects the failure mode, which can result in either higher or lower resistance. The thickness of the shear bands is dependent on the element size. Smaller elements will give thinner shear bands, and consequently more localized softening, which makes the deformation mode highly dependent on element size. This can be seen from the contour plot of the absolute plastic strain, where the model with the coarsest mesh has a significant larger softening zone.

3.1.4 Summary triaxial compression test

The triaxial compression tests have revealed that the Young's modulus is correctly implemented. The cohesive yield strength is a bit underestimated, but it is a small error if sufficient mesh resolution is used. The resistance is affected by the element size and compression speed. Smaller elements will increase the numerical accuracy of the calculation, and it will also produce different deformation modes. The compression speed also affected the deformation mode and consequently the resistance. Lower resistance was measured for the model with slower compression speed due to failure of the non-softening soil. This deformation pattern naturally produced more excessive shear bands as the soil failed in compression (Figure 3-5). The chance for inhomogeneous deformation modes may be reduced by using more boundary conditions such as symmetry plane in order to get the same mode for different element sizes and speeds. However, this was not done in this study. Strain-softening soil behavior was difficult to calculate. The problem is that there are many solutions as a result of different deformation modes. Different element sizes and speeds alter the deformation mode, and consequently where the shear bands are established. This will affect the resistance as localized strain-softening will occur in the shear bands, and the thickness of the shear bands is dependent on the element size. It is possible to control the thickness of the shear band with regularization methods such as non-local strain. But where the shear bands develop are still undetermined, which is also seen in real triaxial tests. We must, for example, know local variations in material properties in order to obtain a unique solution. However, this is not realistic as the variations may be minor and hard to detect or measure. But, it is possible to disturb the solution with small random perturbations to reveal different possible solutions in order to get the right deformation mode. It is therefore still possible to analyze the softening problems, but the interpretation of the solution should be done carefully.

3.2 Oedometer test

The oedometer test was modeled to analyze how the eulerian mesh preformed under high compression in Abaqus/Explicit.

The model is fairly simple, where a cylindrical soil sample is compressed by a plate. The cylinder is constrained for horizontal movement at the sides, and lateral displacement at the bottom. The compression plate is constrained to a reference point which is given a constant velocity during the compression. The height of the soil sample is 0.3 meters, and the diameter is 1 meter (Figure 3-8).

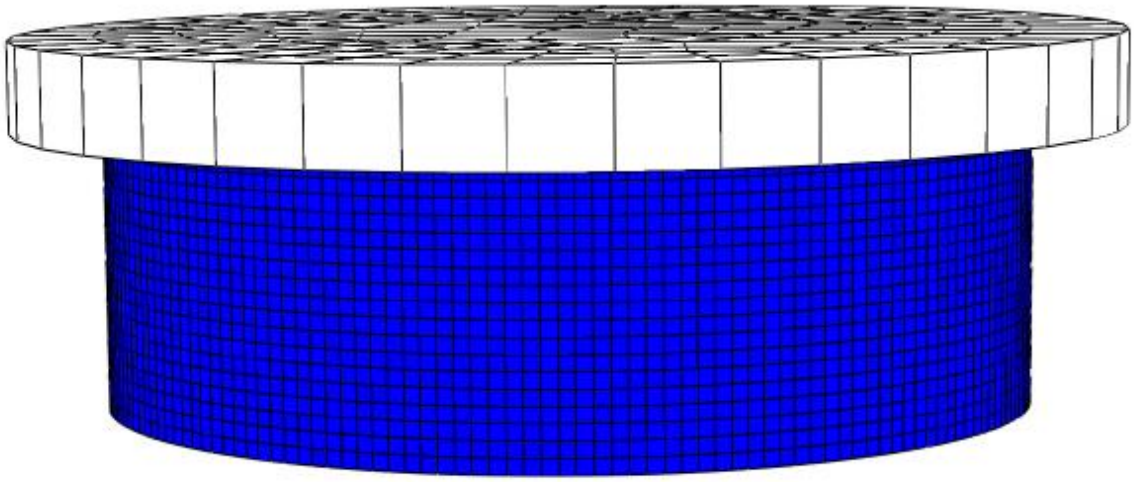

Figure 3-8 Oedometer model

The soil parameters are listed in Table 3.

Young's modulus (E)	1000 kPa
Poisson's ratio (ν)	0.3
Cohesion yield stress (c)	1E7 kPa
Friction angle (ϕ)	0°
Dilatation angle (ψ)	0°

Table 3 Soil properties for oedometer test

3.2.1 Small strain analysis

First, a calculation was done for small strain to verify the finite element model. The element size was 0.017 for this calculation. The speed of the plate was set to 0.0014 m/s. The theoretical solution was calculated using the small strain measure ($\varepsilon = \frac{\Delta h}{h_0}$)

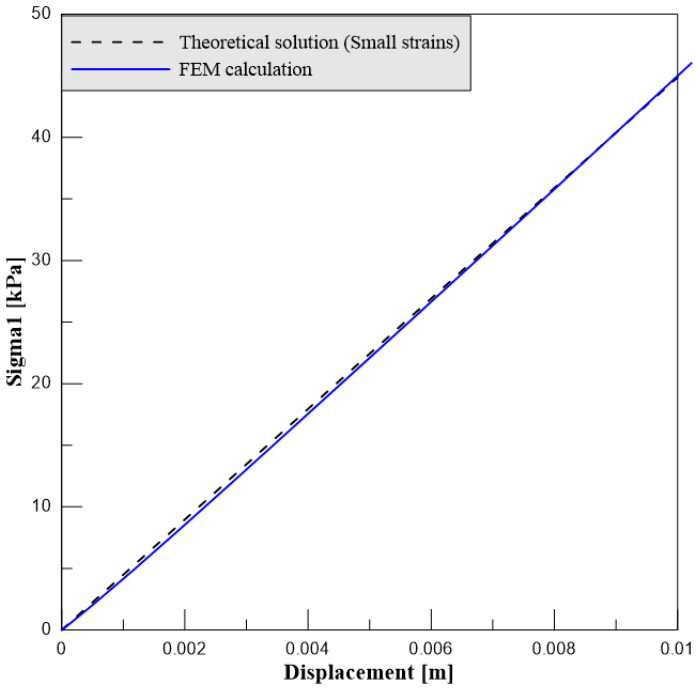

Figure 3-9 Small strain calculation

The result is plotted in Figure 3-9 with the theoretical solution. The model worked well for small strain, with only minor errors.

3.2.2 Large strain analysis

Large strain analysis was performed after this. The true-strain measure was used to hand calculate the resistance. Two element dimensions were used, namely 0.034 and 0.017. The speed of the compression plate is still 0.014m/s.

The resistance functions are plotted in Figure 3-10, with the theoretical solution. Both of the models had problems with calculating the large compression-forces. The model with element size 0.034 deviated from the theoretical solution around 0.13m, while the model with element size 0.017 diverged around 0.19m displacement. It is obvious that modeling full compression in Abaqus/Explicit can be problematic.

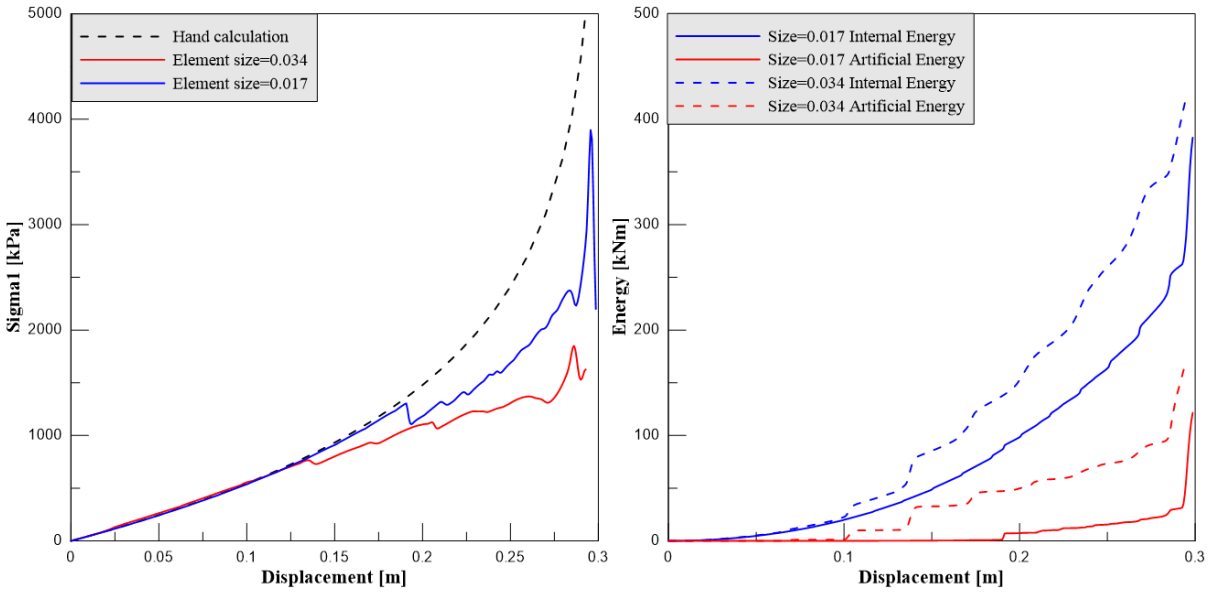

Figure 3-10 Large strain calculations

The artificial energy becomes significantly large when the models start to have numerical problems, as shown in the right picture in Figure 3-10, which display the energy for the models. The internal energy contained around 7.8% artificial energy for 0.19 meters compression in the model with element size 0.017. However, it is not always easy to spot the artificial energy from the resistance function. As the internal energy to the model with element size 0.034 contain 10% artificial energy already after 0.11m compression. So this model was unstable before it was possible to see any divergence from the theoretical solution.

The analysis with element size 0.017 and Poisson's ratio of 0.3 and compression speed of 0.014m/s took around 5 hours to calculate with 8 CPUs, while the similar model with element size 0.034 only used 16 minutes to complete. Further reduction in element size will significantly increase the calculation time. The accuracy of calculations containing large compression forces is often constrained by computational power and time. Finding the right compression speed is therefore important in order to reduce the calculation time.

3.2.3 Compression speed

The compression speed was also subject to investigation. The model with element size 0.017 was used, while the speed was increased from the original analysis.

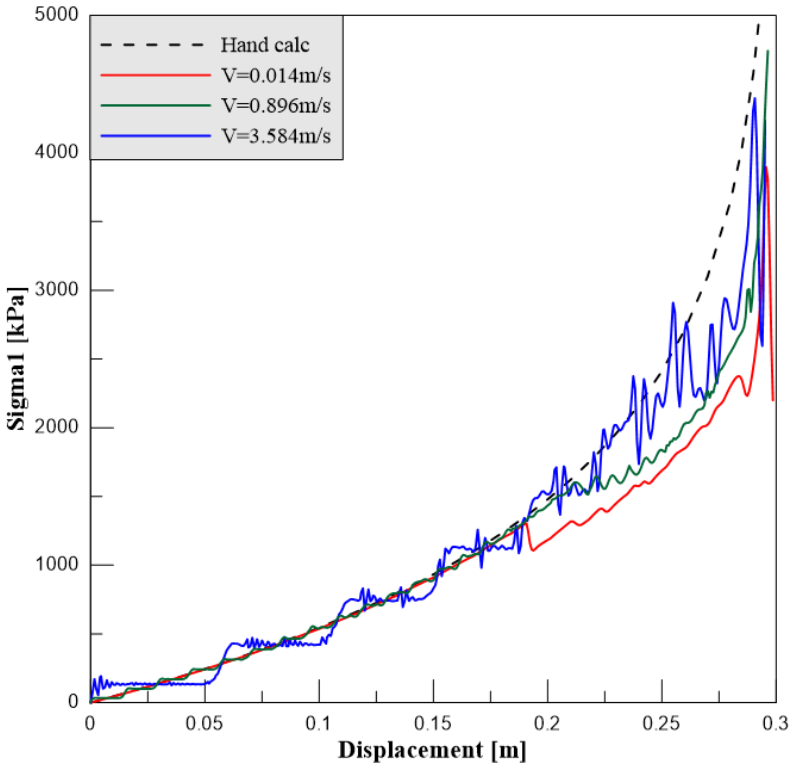

Figure 3-11 Oedometer calculations, subject to different compression speed

The results are plotted in Figure 3-11, and it shows that the oedometer test can withstand a lot higher speed than used in the first calculations (V=0.014m/s). The solution starts to show signs of oscillations at compression speed of 0.892 m/s. Further increased speed leads to severe oscillations. However, the oscillations may be reduced by filtering techniques e.g. by taking the average resistance over a given displacement. This is possible for the model with speed of 0.892m/s, as the resistance oscillated periodic around the right value. For the calculation with element compression speed of 3.584m/s is this more problematic, as the oscillations are larger, and have longer period.

3.2.4 Summary oedometer test

The oedometer test has shown that it is hard to calculate full compression in Abaqus/Explicit. However, the solution is stable up to a certain point which is highly dependent on element size, and consequently a very dense mesh resolution is needed in order to calculate problems with large compression forces. Analyzing problems with large compression forces is therefore often constrained by computational power and time. The compression speed affected mainly how much oscillation that occurred in the resistance function. Too high speed will lead to inaccurate results, as the oscillation becomes too large to filter out. Finding the limit speed for which it is possible to filter out the oscillations and obtain the correct resistance is therefore a good way to reduce the calculation time.

3.3 T-Bar penetration

The T-bar penetration test is modeled in Abaqus/Explicit to study how the solution is affected by the element density and the penetration velocity. The theoretical value for the T-bar factor is based on a plastic solution in plane strain. The plane strain assumption is justified by that the horizontal cylinder is long enough for the resistance at the end to be neglected. The penetration of a T-bar is in some way similar to a spudcan penetration after back-flow is initiated. Because of that an object is being pushed through the soil, and the soil flow around the object. It is expected that slower penetration rate and denser mesh resolution will lead to convergence to the theoretical value of 12. However, a higher value is expected since the theoretical value is based on plastic solution, whereas this is a dynamic calculation.

The soil is modeled with only one element in width, as the end effect is neglected in the theoretical solution. The height of the soil is 0.6 meter whereas the 0.05 meter of the top is empty, and the length is 0.4 meters. The T-bar has a diameter of 0.05 meters, and it is placed 0.215 meters into the soil as seen in Figure 3-12. Only half of the problem is modeled because of the symmetry.

Figure 3-12 T-bar penetration model

3.3.1 Mesh convergence

First a mesh convergence test was performed in order to study the effect of the element size for soil-flow around the T-bar. The speed of the T-bar was not studied in these analyses, and it is not the same for all the models. It might, however, have been more efficient to study the speed of the T-bar in advance in order to know which speed to use to avoid oscillations in the result.

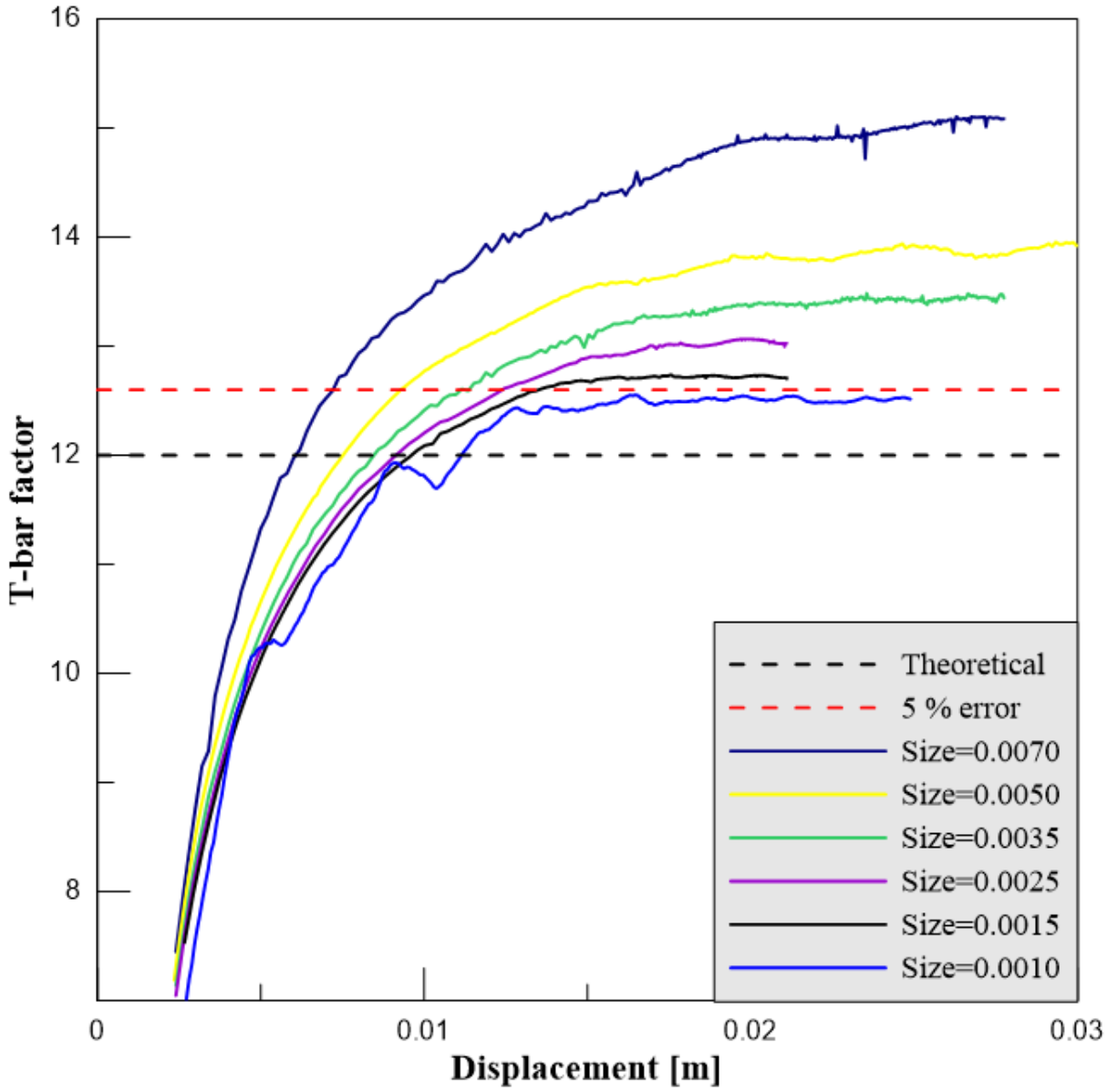

Figure 3-13 Mesh convergence for the T-bar test

The calculations show that the T-bar factor is significantly affected by the element size. Convergence to a constant value was not possible as the calculation time become too great for smaller element size. However, the models with the smallest element size performed well, and the error for element size 0.0010 is less than 5 %.

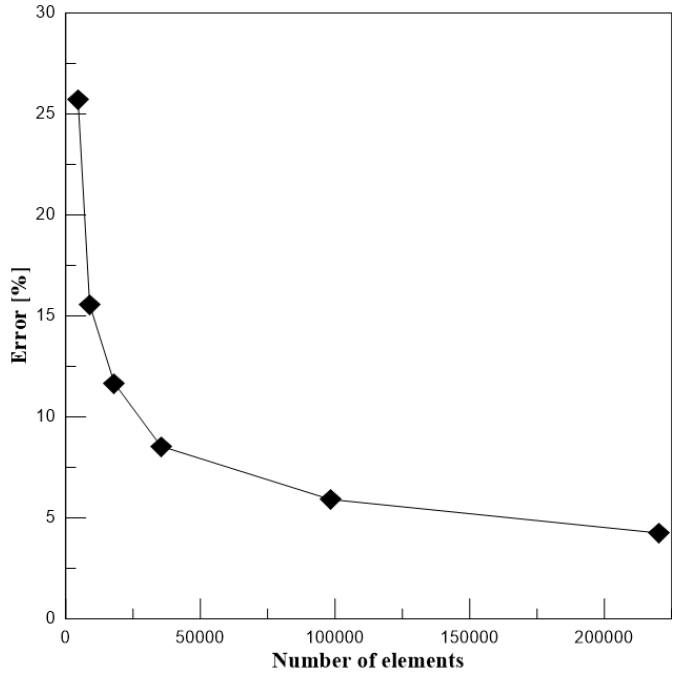

Figure 3-14 Error vs Nr. of elements

Figure 3-14 illustrates the error plotted against the number of elements, and provides a better understanding to why not further mesh refinements was done. The error does not decrease significantly when the element size is reduced from 0.0015 to 0.0010, but the number of elements increases a lot. A higher speed was used on the model with element size 0.0010 in order to keep the calculation time acceptable low. This led to some oscillations in the results as seen in Figure 3-13. Further reduction in element size would increase the number of elements extremely, for example an element size of 0.0005 would give 2,642,400 elements.

The flow around the T-bar displays why the models with denser mesh give less resistance and therefor more accurate results. In Figure 3-15 is the flow pattern of the model with element size 0.0015 displayed over the model with element size 0.0070. A smaller amount of soil flow around the T-bar in the model with denser mesh, and consequently less resistance is measured. The edge of the soil that flows around the T-bar is located 0.05 meters from the side of the T-bar for element size 0.0015, while the distance is 0.07 meters for element size 0.0070. The problem is that when the T-bar penetrates only parts of the element below the T-bar, the displacement of this material becomes downwards with the T-bar. This will increase the effective diameter of the T-bar, and consequently make the fracture zone too large. The shear band which is established along the edge of the soil flow is also narrower and more distinct for smaller element size (Figure 3-16), which will result in lower resistance.

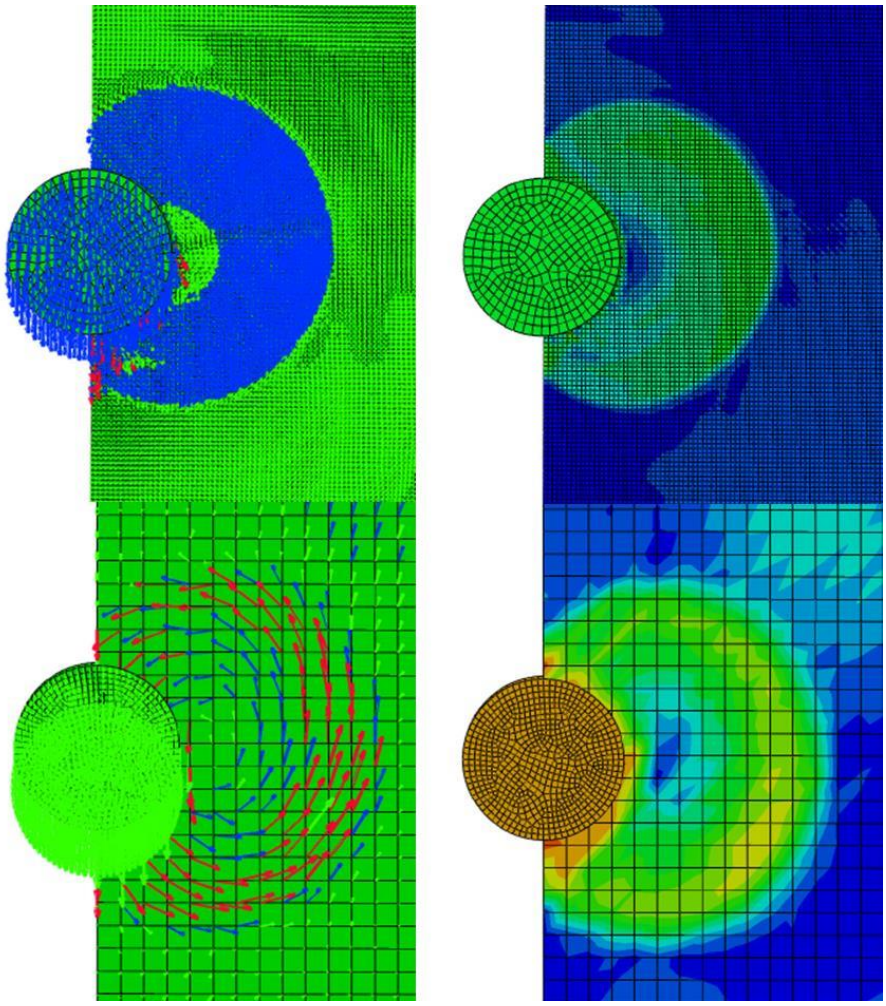

Figure 3-15 Flow: element size 0.0015 and 0.0070

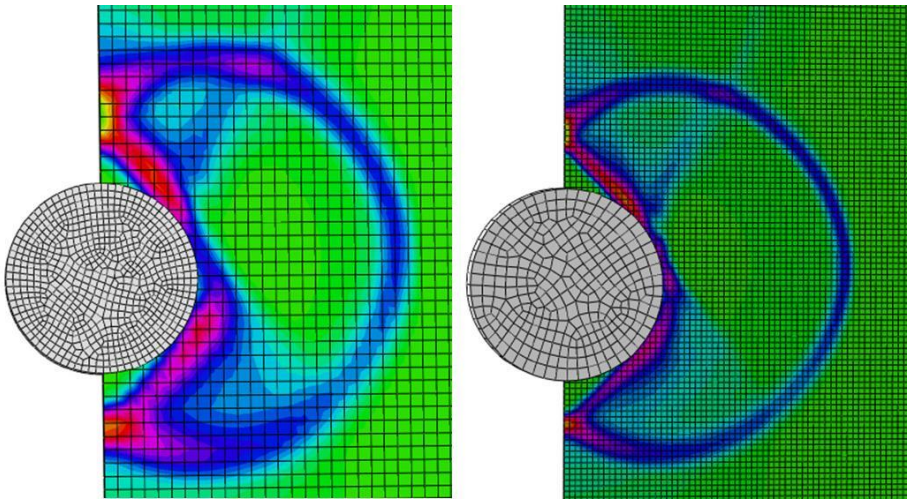

Figure 3-16 Shear bands, Element size 0.0035 and 0.0015

3.3.2 Speed convergence

The mesh convergence test indicated that the penetration speed affected how much oscillation that occurs in the results. It is also of interest to see if the bar factor changes for increased speed, or if the oscillations may be smoothed out (in order to get the right value). This is important to know for the spudcan penetration test, as the deformations are much greater, and increased speed may reduce the calculation time significantly. The model with element size 0.0015 was used for this study, and the speed is constant for each analysis. Several different speeds of penetration were tested, and a selection of two of them is shown in Figure 3-17. The rest of the calculations are given in Appendix A.

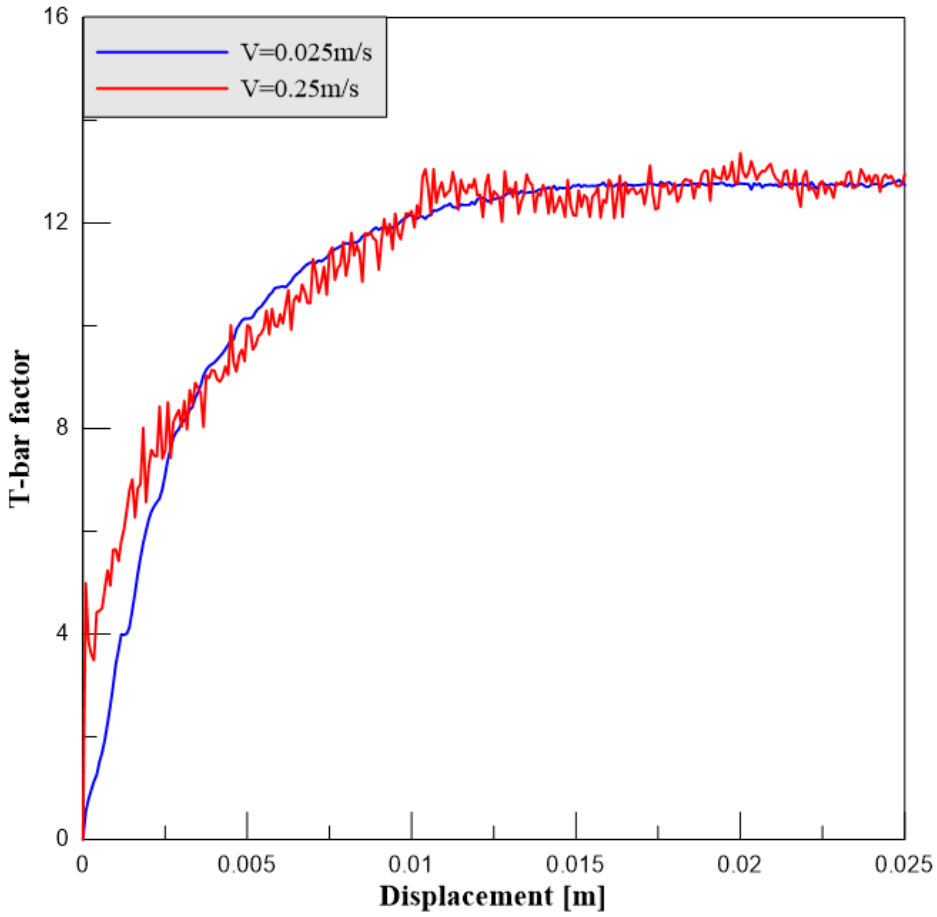

Figure 3-17 Speed convergence

The result indicates that the resistance is more influenced by the speed at small deformations than large deformations. The fast calculation seem to stabilize around the right value as the deformation become larger (>0.005 meters). And a T-bar factor with only a minor error is possible to obtain by filtering out the oscillations in the resistance for the fast calculation, for example by taking the average resistance over a given displacement. This approach may be used for the spudcan penetration analysis, as the deformation is large. However, it will lead to some errors if the resistance changes a lot during the penetration which may be the case around the punch-through depth.

3.3.3 Strain-Softening

Strain-softening was introduced to the model with element size 0.0025. The model was chosen due to the low calculation time and relatively accurate results (8.6 % error). Strain-softening was introduced in the same way as for the triaxial compression test. The sensitivity is 2 for two of the models (A=2) while the absolute plastic strain for which the residual strength occurs is 40% and 80% (μ=0.4, μ=0.8). Two similar calculations were done, with a sensitivity of 1.33 ($c_{residual} = 0.75c_u$).

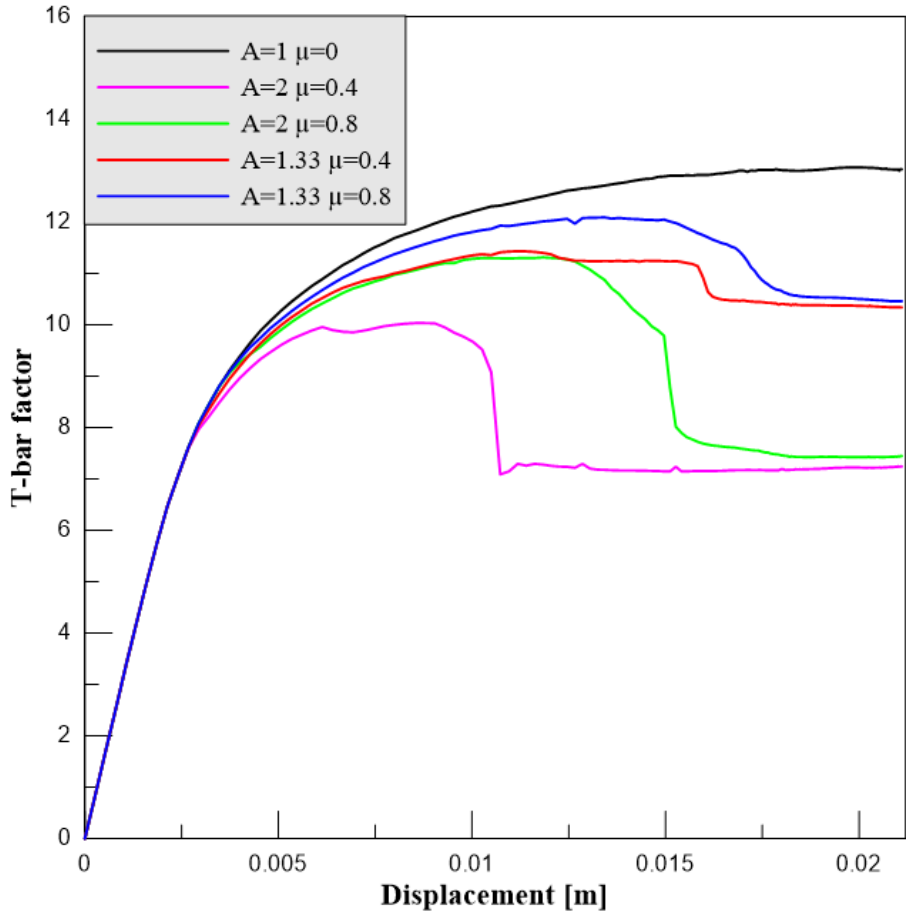

Figure 3-18 T-bar penetration with strain-softening

The results are shown in Figure 3-18. The models with μ=0.8 produced a slightly higher T-bar factor. As seen in Figure 3-20, the strain-softening is localized in the shear bands. This results in reduced stresses in the rest of the soil, as seen in Figure 3-19. The T-bar factor is reduced by 44.4% and 42.8 % for namely μ=0.4 and μ=0.8 when the sensitivity is 2. While the reduction is 20.6% and 19.7% for μ=0.4 and μ=0.8 when the sensitivity is 1.33. The strain-softening of the soil is localized in the shear bands, which is probably the cause for that the T-bar factor is reduced less than the cohesive yield strength (50% and 25%). However, this is not necessary misleading for the test result, as localized strain-softening will occur in a real test with clay that have a sensitivity larger than 1. But the reduction is also affected by the element size, because the thickness of the shear bands are determined by the element size.

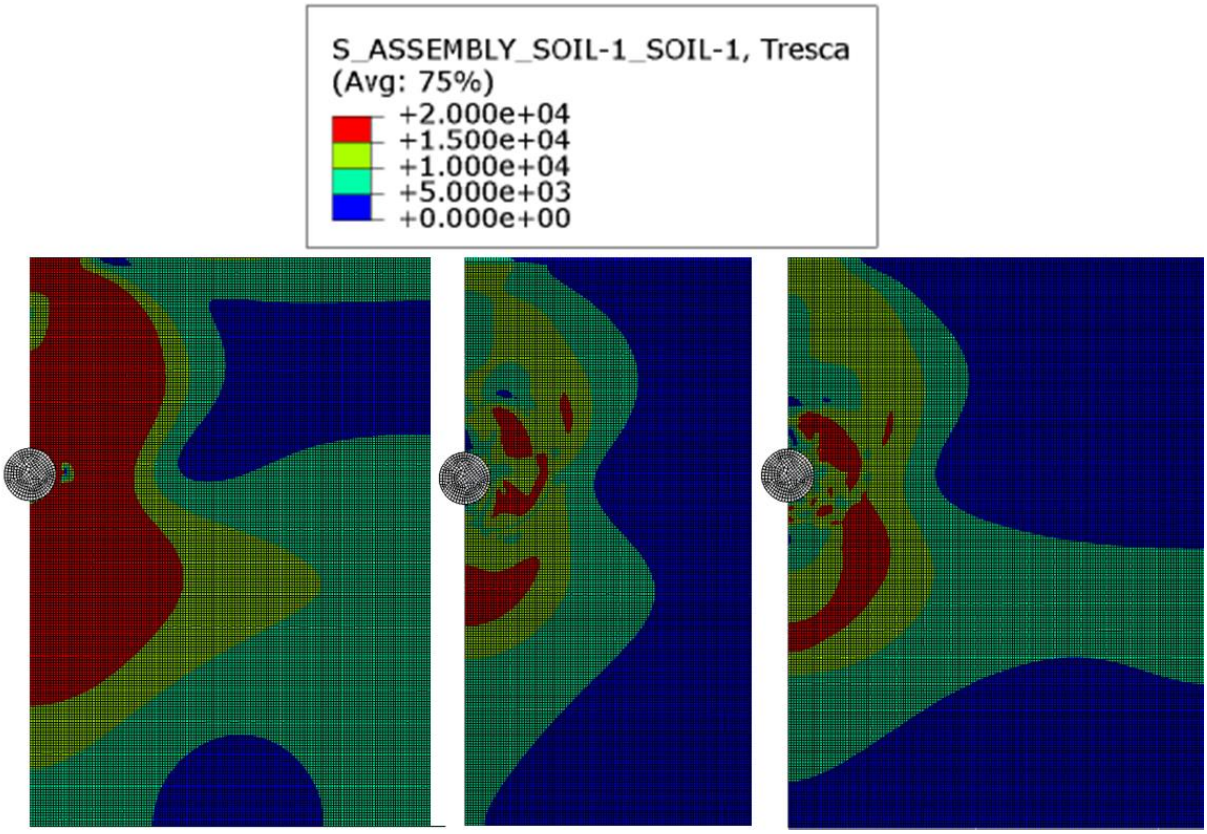

Figure 3-19 Tresca stress. Picture from left: A=1 μ =0, A=2 and μ =0.4, A=2 and μ =0.8

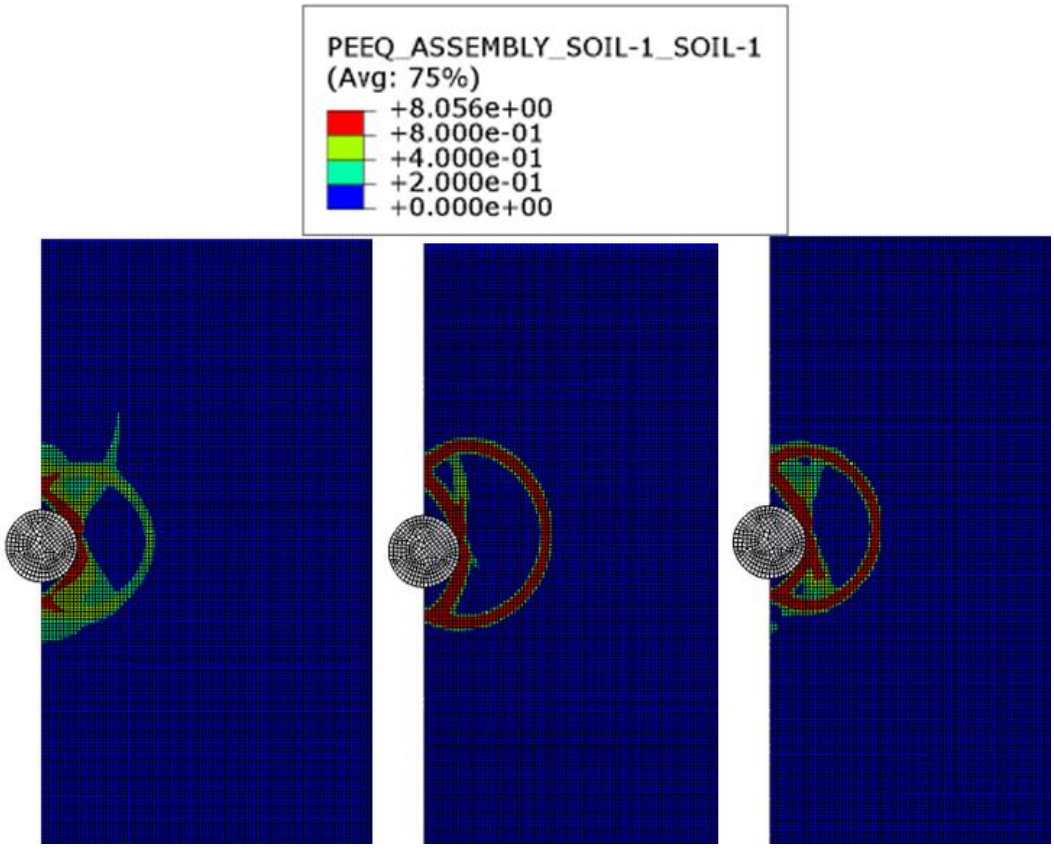

Figure 3-20 Equivalent plastic strain. Pic from left: A=1 μ=0, A=2 μ=0.4, A=2 μ=0.8

3.3.4 Summary T-bar test

The T-bar tests have shown that the resistance during penetration is greatly affected by the element size. Reduced element size results in less soil flowing around the T-bar. It will also make the shear band more distinct and thinner, which will reduce the resistance. The speed of the penetration had only a small effect on the T-bar factor, but it did lead to oscillations in the result. However, it is possible to filter out the oscillations in order to obtain the right value. The eulerian elements worked in general very well for flow around the T-bar, but a dense mesh is needed in order to get the right resistance. Strain-softening gave apparently reasonable result, but the T-bar factor was reduced less than the cohesive yield strength. It appeared to be because the strain-softening only happens in the shear bands. Calculations that include strain-softening soil should therefore be interpreted carefully, as the thickness of the shear bands is determined by the element size. These tests show again that the accuracy while using the CEL method in Abaqus/Explicit is constrained by computational power and time. It is, however, possible to get close to the theoretical solution for the T-bar test.

Chapter 4. Spudcan penetration in single-layer clay

The first analysis on spudcan penetration was executed in order to verify the method. The soil is weightless in this case, so that none back-flow occurs. The spudcan is modeled as a flat cylinder with a rough base. The diameter of the cylinder is 15 meters. All the penetrations are preformed undrained, and poisons ratio of 0.495 is used. The cohesive yield strength is 10kPa for all the soil. Only 45 degrees of the problem is modeled, and symmetry boundary conditions are used on the sides. The height of the initially active elements (soil) is 3.5D=52.5 meters, while the radius is 2.5B=37.5 meters. This is the same dimensions that Sindhu Tjahyono used (Tjahyono, 2011). Approximately 228 000 elements were used, and a penetration rate of 1m/s. The stable time increment for this calculation was 1.7267E-04 sec, and the calculation took 9 hours with 8 CPUs.

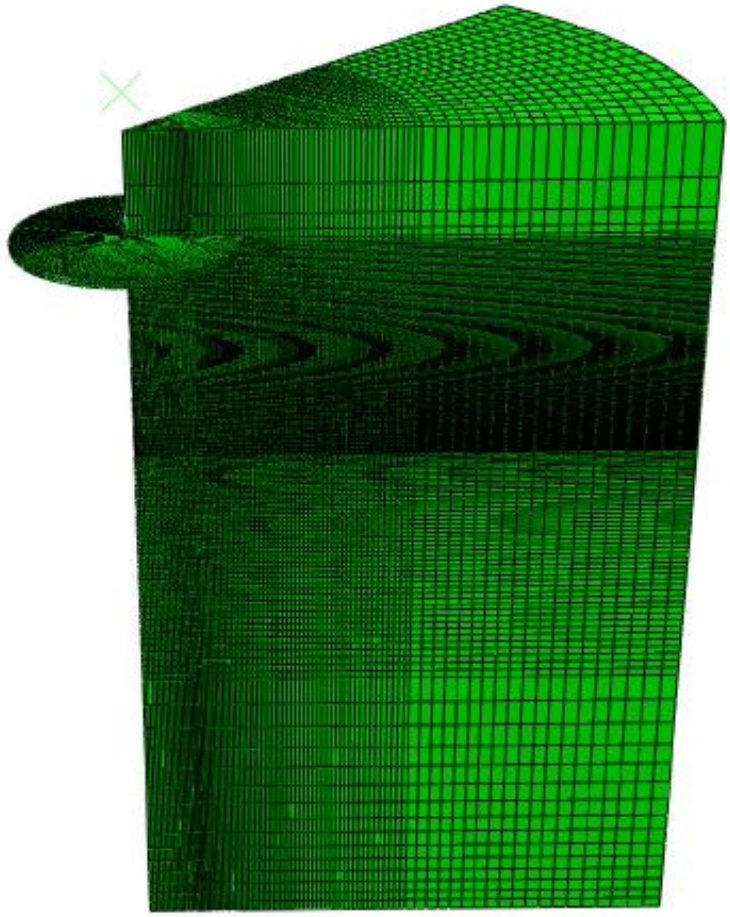

Figure 4-1 Mesh: single-layer penetration

The reaction force was measured, and oscillations were filtered out. The bearing capacity factor were calculated by $N = q/c_u$. The results were compared with Martin and Randolph's lower and upper bound solutions (Martin, C.M. and Randolph, M.F., 2001).

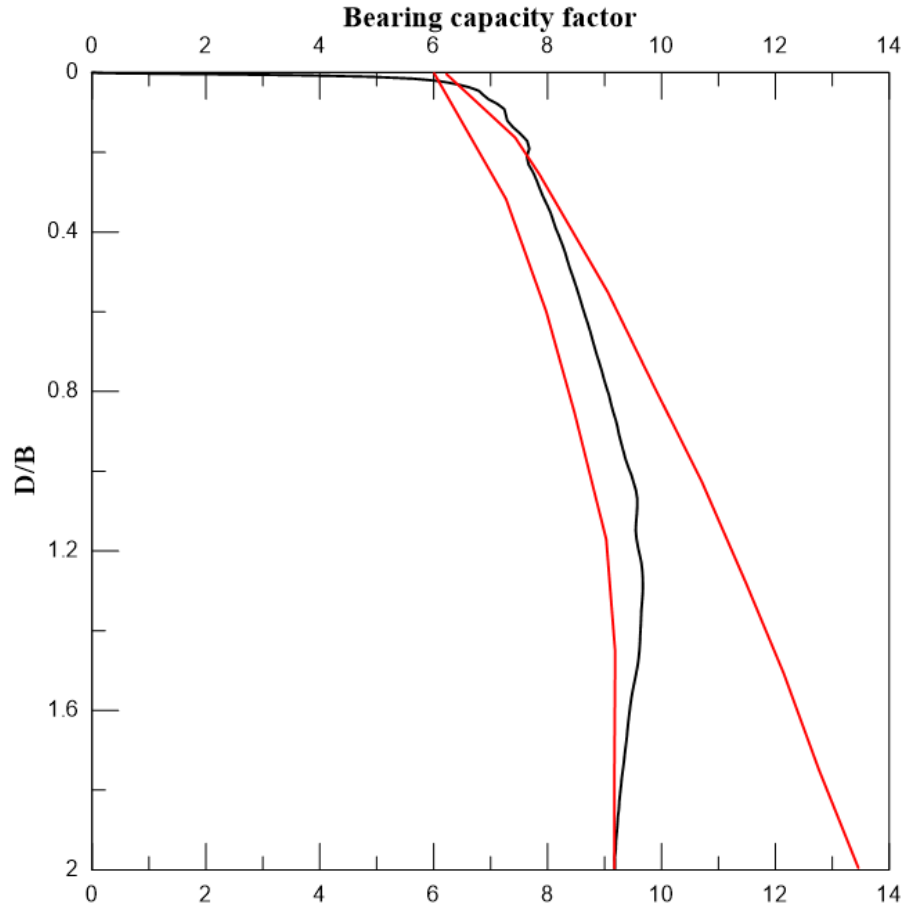

Figure 4-2 Bearing capacity factor for single-layer clay

The calculation is in reasonable agreement with Martin & Randolph's bearing capacity theory. The result shows some error for shallow penetration, which is likely due to the dynamic inertia effects, or not small enough elements. The kinetic energy is more that 10% of the internal energy for D/B<0.01. However, it is under 3% of the internal energy for D/B>0.1, so it should not affect the result too much after that depth. The result is otherwise within the upper and lower bound solution to Martin & Randolph, so the model seems to perform with reasonable accuracy. The FEM calculation is also numerical stable for the whole analysis, as the artificial energy is at maximum 2.43% of the internal energy (end of the penetration).

Chapter 5. Spudcan penetration in two-layered clay

The object was to recalculate Sindhu Tjahyono's numerical models which included strain softening. The limit cases did not include strain softening, but was either pre-softened or nonsoft materials. These cases were subject to comparison with the theoretical solutions.

Tjahyono modeled 45 degrees of the problem, and used symmetry boundary conditions. The height of the soil was 3.5B and the width 2.5B, and the penetration rate was 1 m/s. Approximately 228,000 elements were used in Tjahyono's study. Similar dimensions and penetration rate will be used in this study. However, a somewhat different mesh will be used, but approximately the same amount of elements (225,000). The calculations which does not include strain-softening should have only small errors if sufficient fine mesh is used. But the models that include strain-softening are expected to show larger differences, because the element size appeared to affect the strain-softening behavior (Triaxial compression test and T-bar test). Two cases from Sindhu Tjahyono work will be calculated, where the difference is the H/B ratio, which is namely 0.5 and 1. The result from Tjahyono's analysis is presented in Figure 5-1.

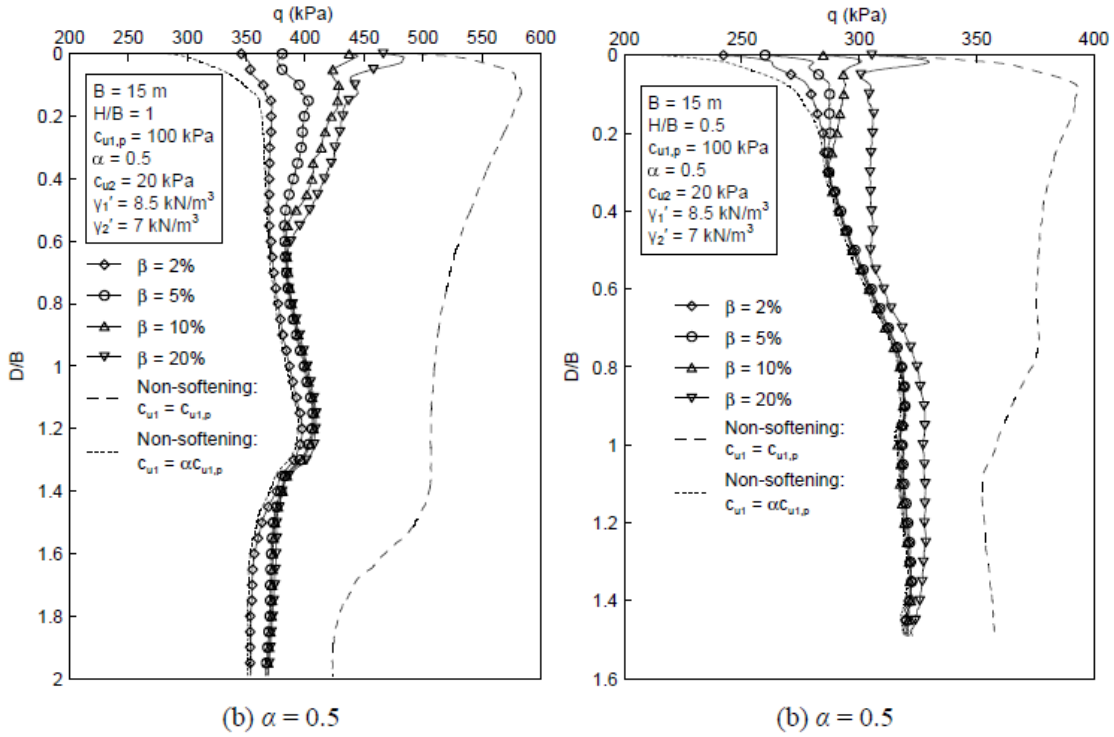

Figure 5-1 Sindhu Tjahyono's results (Tjahyono, 2011)

The cohesive yield strength of the upper layer is 100kPa, and 20kPa for the lower layer. The effective soil weight is 8.5kN/m^3 for the upper layer, and 7 kN/m^3 for the lower layer. Strain-softening is introduced in the same way as in the triaxial test, and μ is varied from 20% to 2%. Only the upper layer is subject to strain softening, as this is argued by Tjahyono to be the layer that normally has a strain-softening behavior. The sensitivity is 2 for both cases.

5.1 H/B=1

The mesh used for H/B=1 is shown in Figure 5-2. Approximately 225,000 elements are modeled, as this was close to what Tjahyono used. A mesh convergence test is not performed because the calculation time is already large for this model, and Tjahono's research showed that approximately 228,000 elements worked well. However, the FEM model used in this study have smaller elements in the top and layer and larger elements in the bottom in order to study the effects of the element sizes. The critical time step was 5.034E-05 sec, and the calculation time was approximately 19 hours with 8 CPU's.

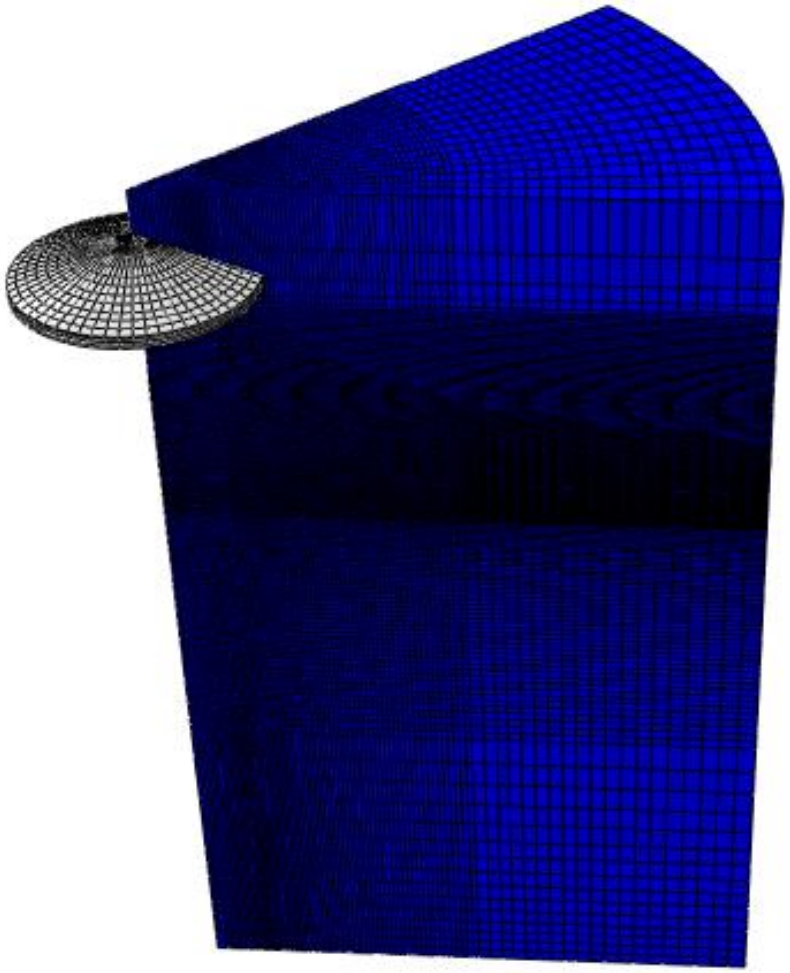

Figure 5-2 Mesh: two-layered clay

5.1.1 Upper limit case

First, the case with no strain-softening was calculated, where the cohesive yield strength in the upper layer is 100kPa, and 20 kPa in the lower layer. The Young's modulus is $500c_u$, and the effective soil weight is 8.5kN/m^3 for the upper layer and 7kN/m^3 for the lower layer. The diameter of the spudcan is 15 meters.

The "decimateFilter" function in Abaqus/Explicit was used to filter out the oscillations in the test data. The results are shown in Figure 5-3, where the spudcan resistance is plotted against the normalized penetration H/B. It is evident that the oscillations are large in the beginning of the penetration. However, the result is not necessarily inaccurate. After filtering out the oscillations and comparing the resistance with Tjahyono's result, we get the result as shown in Figure 5-4. The result from the FEM analysis is normalized with Tjahyono's result so that they start at the approximately same resistance for D/B=0. The result seem to be fairly good, in the sense that it does not deviate much from Tjayhono's FEM calculation, with the exception of the dynamic oscillations at the beginning, and at the end where backflow initiates. The deviation is at maximum around 25 kPa, for both the beginning and end of the penetration. The back-flow is initiated at around D/B=1.40, and the flow pattern and material boundaries are shown in Figure 5-5. The right picture shows the upper material in red and the lower material in blue. The eulerian mesh seem to preform very well in managing the boundaries, as we can see the upper layer is pushed into the lower layer. The problems at the end may be because the element size in the lower layer is not small enough. However, the artificial energy is low compared to the internal energy for the whole penetration (max 2.02% of the internal energy) so the calculation is numerical stable. The kinetic energy is also low, whit the exception of very shallow penetration (D/B<0.08). A contour plot of the upper layer at the end of the penetration is shown in Appendix C Spudcan penetration two layered clay.

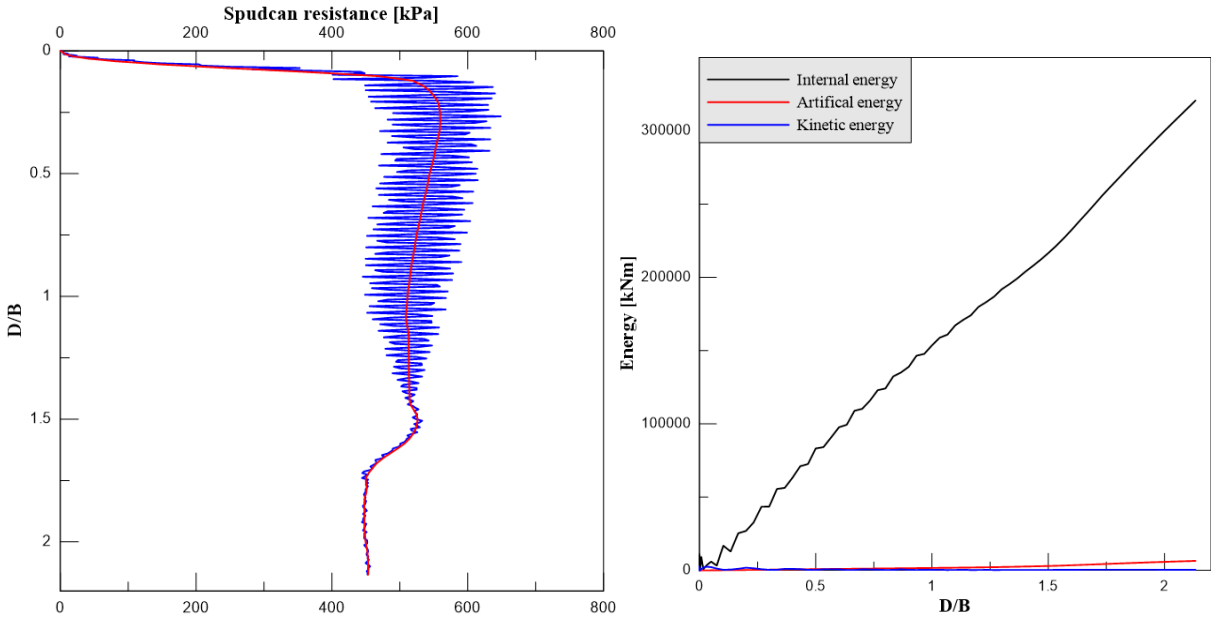

Figure 5-3 Response filter and energy

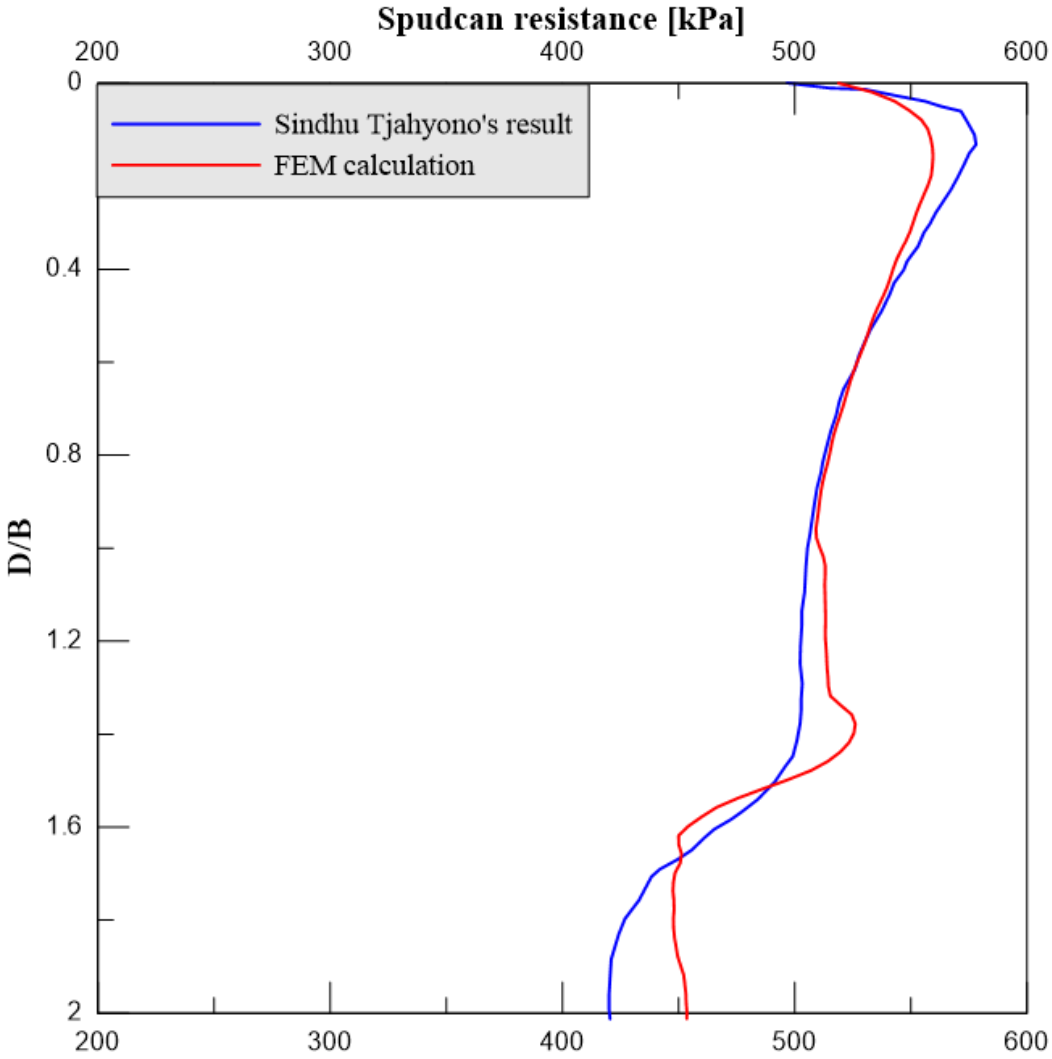

Figure 5-4 Spudcan resistance non-soft material, compared with Tjahyono's result

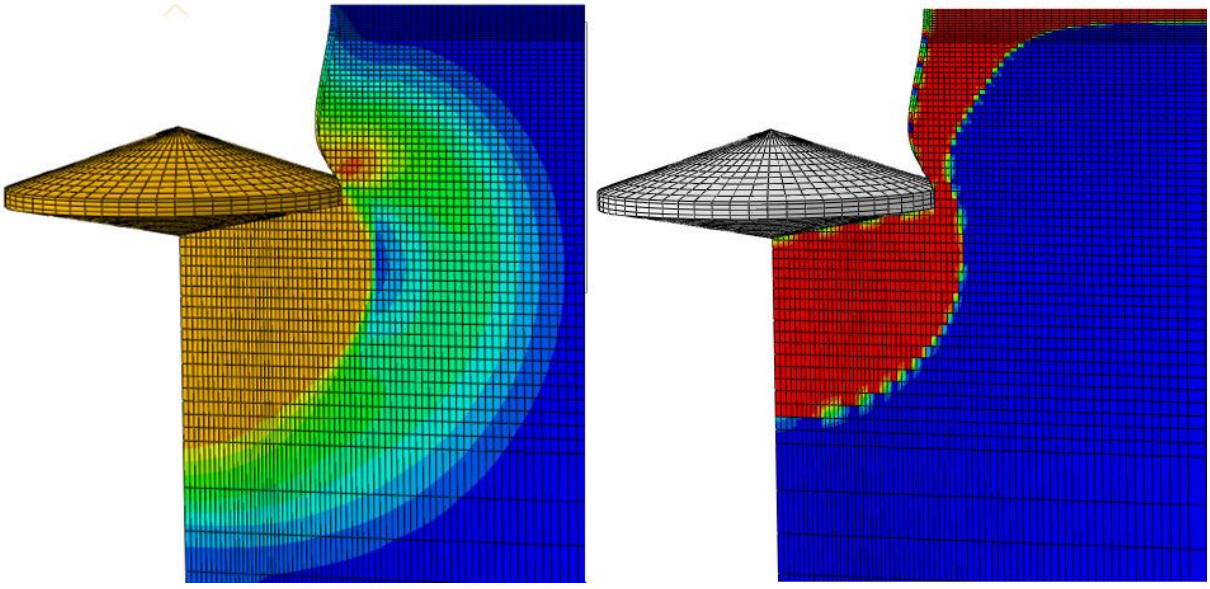

Figure 5-5 Flow pattern and material boundaries at initiation of back-flow ($D/B \approx 1.4$).

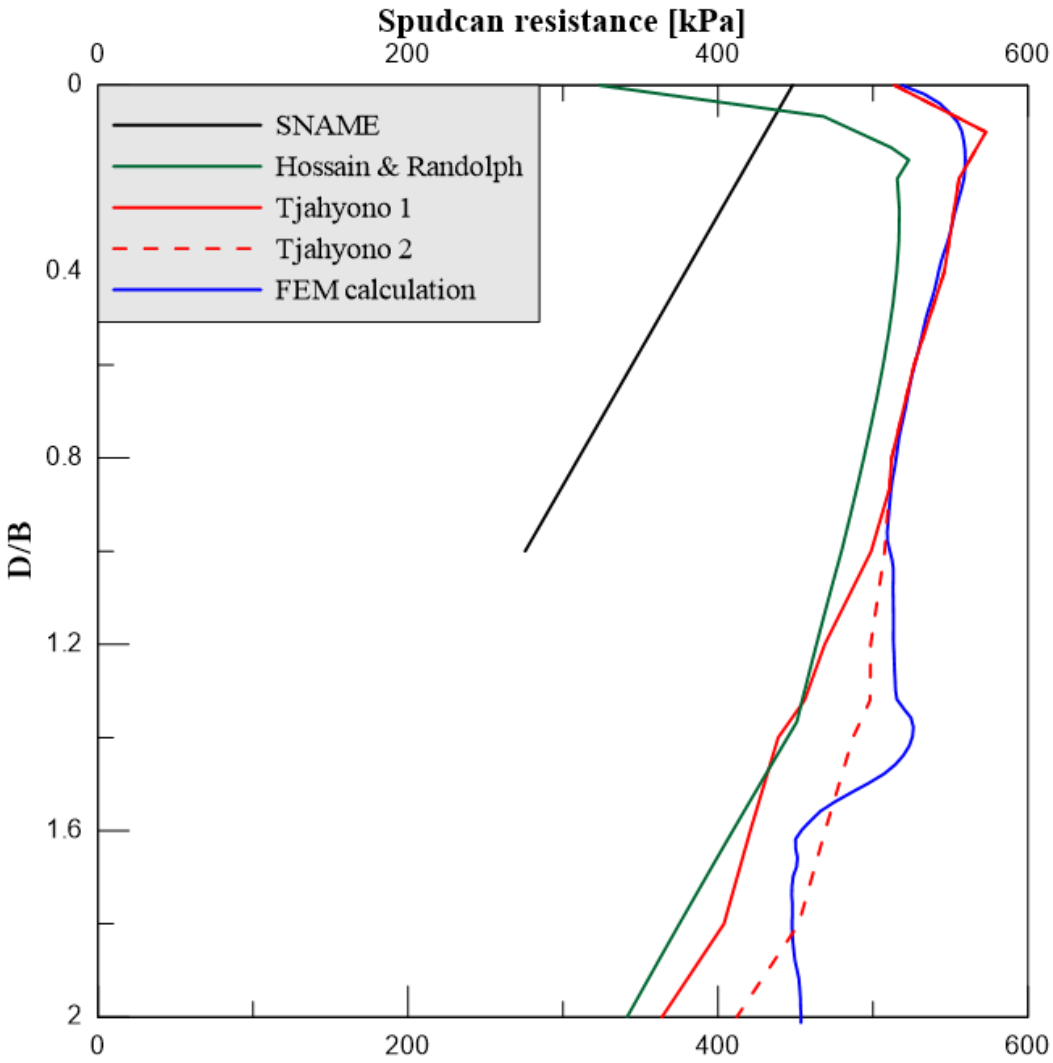

Figure 5-6 Comparison of spudcan resistance with hand calculations

The result from FEM calculation was also compared with the theoretical solutions from SNAME, Hossain & Randolph and Tjahyono in Figure 5-6. The SNAME method overestimates the potential for punch-through, and underestimates the spudcan resistance. The reason for the apparently bad performance of SNAME method is because of the whished-in-place approach. This case involves a large reduction in the cohesive yield strength from the upper to the lower layer, and SNAME will consequently underestimate the resistance and overestimate the potential for punch-through as it does not account for the geometric chances in the soil. The much stronger upper layer will be pushed into the lower layer, and this deformation will increase the spudcan resistance and reduce the potential for punch-through. Hossain & Randolph's method performed better, but is still underestimating the spudcan resistance if we compare to the FEM calculation and Tjahyono's result. The FEM calculation is close to Tjahyono's theory, but has some problems at the end where back flow initiates. It was problematic to calculate the depth of initiated back-flow with Tjahyono's theory. The FEM calculation indicated that the back-flow would start in the lower layer. Also taking the average cohesive yield strength over the depth and comparing with the overlaying pressure ($\frac{\gamma D}{2}$) indicated this. But $\frac{H}{B} \geq \left(\frac{c_{u1}}{\gamma_1' B}\right)^{0.55}$ which suggested from Tjahyono's theory that the cavity

depth was within the upper layer. This was a confusing point as the back-flow clearly started in the lower layer. The second equation for cavity depth was therefore used for Tjahyono 2, which was somewhat closer to the FEM calculations. The depth of initiated back flow was then calculated to D/B=1.32, which was close to Hossain & Randolph's theory (D/B=1.37), and the FEM calculation ($D/B \approx 1.40$). In Tjahyono 1 were the first equation used, and the depth of initiated backflow become D/B=0.87. The resistance is dependent on the element size for flow around an object as shown in the T-bar test, and from the comparison with Tjahyono's numerical and theoretical work is it possible to conclude that the elements are too large in the lower layer. However, the error was within acceptable range, and further reduction in element size would increase the calculation time which was already relatively long. The same mesh was therefore used for the rest of the calculations.

5.1.2 Lower limit case

The same calculations were then done for the case where the upper layer is pre-softened, which means that the cohesive yield strength is equal to 50kPa in the upper layer from the beginning (no strain-softening behavior). The same mesh was used for this model. The resistance plotted with Tjahyono's result is shown in Figure 5-7. This model performed better in the beginning of the penetration compared to the upper limit case, which might be because the upper layer has less strength. The FEM calculation still overestimated the resistance in the lower layer as soil backflow was initiated at $D/B \approx 1.05$. However, only parts of the soil flow on top of the spudcan, and it is a gap between the spudcan and the soil at the edge of the spudcan (Figure 5-8). This may be because of the element size is too large and speed of the penetration too high to give the soil time to deform properly. The material boundaries is otherwise well managed (Figure 5-9). The error at the end of the penetration (D/B=2) is approximately 8.6% (30kPa).

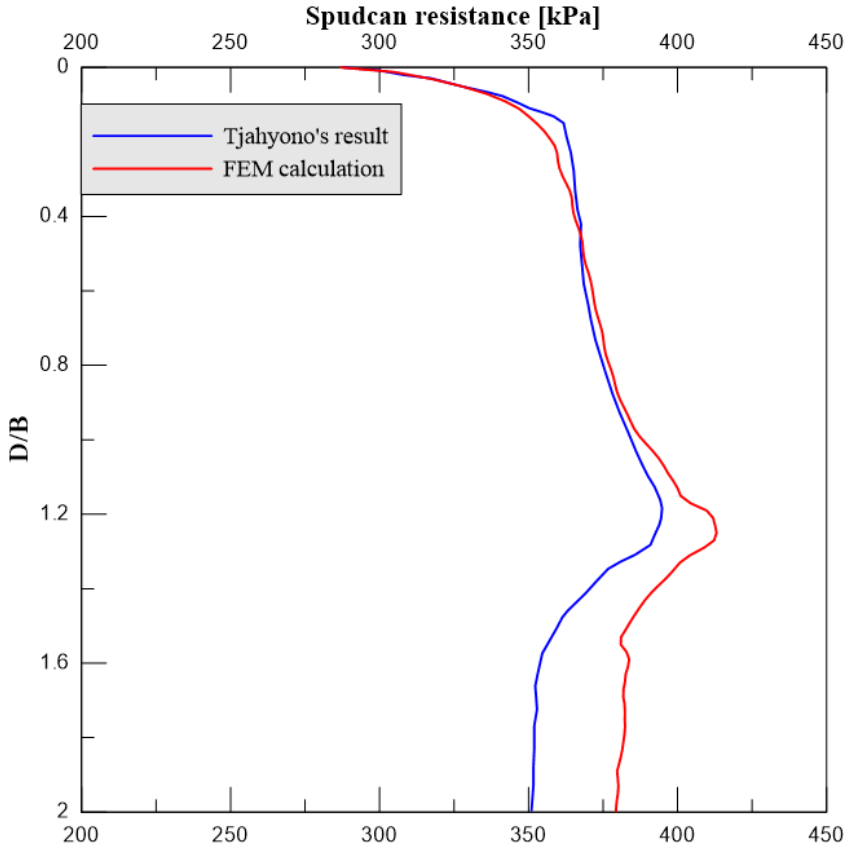

Figure 5-7 Spudcan resistance in full-softening material, compared with Tjahyono's result

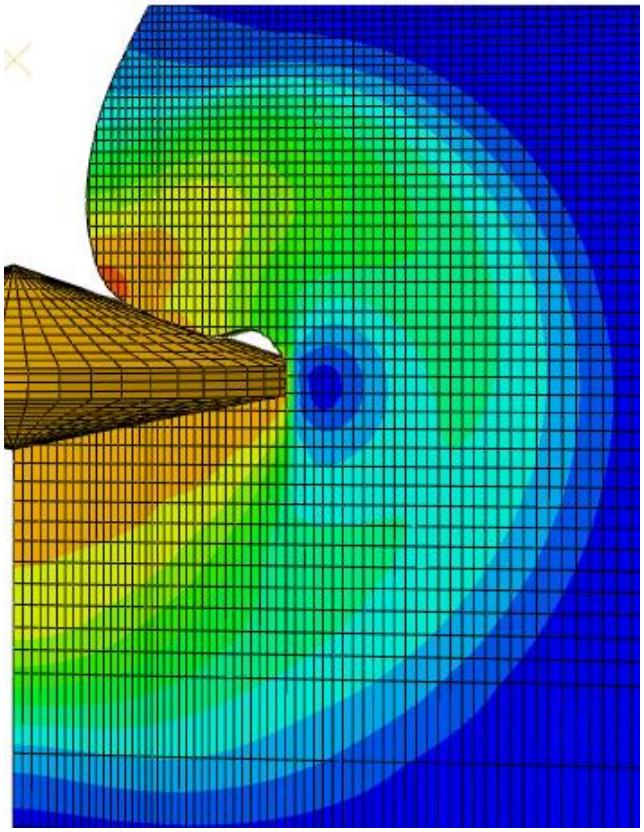

Figure 5-8 Soil-flow $D/B \approx 1.6$: Full softening

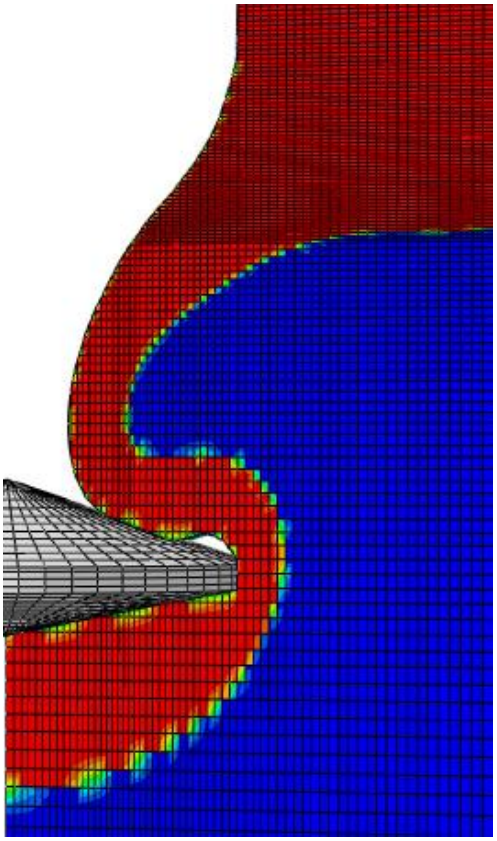

Figure 5-9 Material boundaries $D/B \approx 1.6$

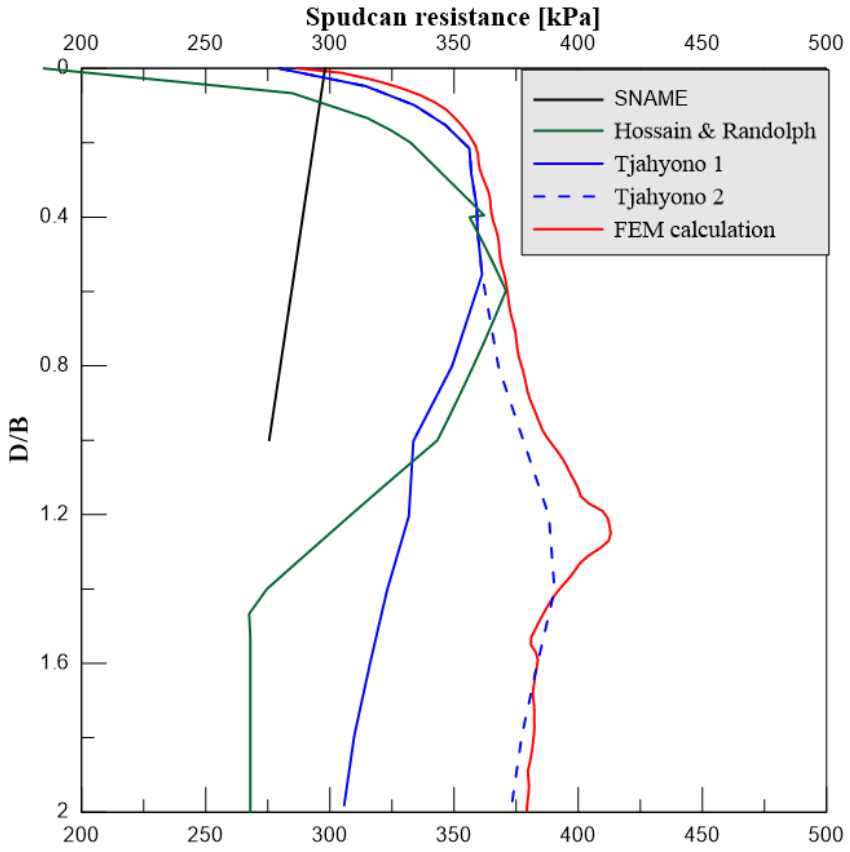

Figure 5-10 Comparison of spudcan resistance with hand calculations

The comparison with the theoretical solutions was also done for this case, and it is evident that SNAME still underestimate the resistance. But it does not show the same punch-through danger, mainly because the upper layer is weaker, and the reduction in spudcan resistance is therefore less. Hossain & Randolph's method was a bit more problematic to calculate in this case, as the cavity depth (depth of initiated backflow) was harder to find. Both the equations for calculating backflow gave values in the upper layer, namely D/B=0.6, and D/B=0.97. The first equation was used, because the second equation is only valid for $d_s > H$. The reduction in spudcan resistance becomes too large for Hossain & Randolph's method compared to the FEM calculation and Tjahyono's theory. This is possible due to the fact that the FEM model does not get full backflow, as only part of the spudcan get covered in soil (Figure 5-8). While Hossain & Randolph's method assume that the whole spudcan get covered in soil after backflow is initiated. For Tjahyono's method are two results plotted, and the difference between them are the equations used for backflow depth. Tjahyono 1 have backflow depth of D/B=0.6, and Tjahyono 2 backflow depth of D/B=1.24. It is evident that Tjahyono 2 fits better with the FEM calculation. However, $\frac{H}{B} \geq \left(\frac{c_{u1}}{\gamma_1' B}\right)^{0.55}$ for this case too, and Tjahyono 1 should therefore be the right result. The FEM calculation seems therefore to overestimate the depth of backflow compared to the theoretical solutions. The FEM calculation also had some problem with calculation the backflow mechanism, as only part of the spudcan got covered in soil.

5.1.3 Strain-Softening

Finally, strain-softening was implemented in the spudcan penetration test. The strain-softening was introduced in the same way as for the triaxial compression test. Only the upper layer was subject to softening. The sensitivity of the soil was 2, which means that the softened soil have half the strength of the original soil. The absolute plastic strain for which the reduced cohesive yield strength was established varied from 2% to 20%. It was expected to get a different result than Tjahyono, as the element size was different, and as we established from the triaxial-compression test, the strain-softening is highly dependent on element size. The calculation time varied from approximately 22 hours to 31 hours. It did not appear to be any connection with the material model and calculation time, as μ=10% gave the shortest and μ =5% the longest calculation time. The upper bound solution ($c_{u1} = 100kPa$) and lower bound solution ($c_{u1} = 50kPa$) were also plotted in the result.

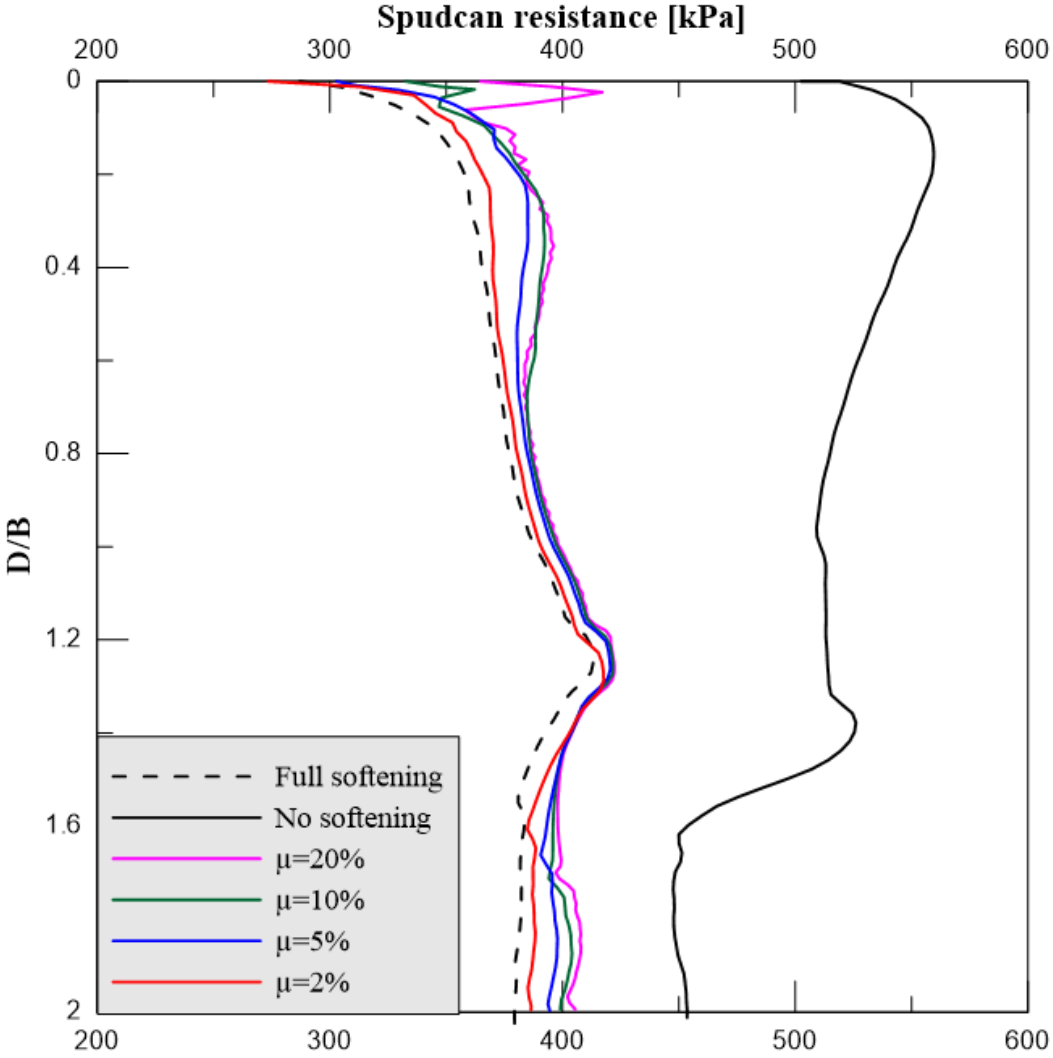

Figure 5-11 H/B=1. Spudcan resistance with strain-softening behavior

The results are plotted in Figure 5-11. It is evident that the different in spudcan resistance between the softening calculations are much smaller for this analysis compared with Tjahyono's results (Figure 5-1). All the calculations are pretty similar to the lower bound solution. It is suspected that this is a result of smaller elements in the top layer compared to Tjahyono's model. The shear band thickness will therefore be narrower, which will reduce the resistance as the strains become more localized. It also seems like the shear bands are established faster in the smaller elements. The strain-softening behavior has less effect when the shear bands are established. This is due to the fact that the strains in the shear bands are much greater than the absolute plastic strain for which the soil is softened (μ). It can be seen from Figure 5-12 that the shear bands are established at relative shallow depth for the strain-softening case with μ=20%. And the effect from μ is clearly smaller compared to Tjahyono's result. The models with μ=10% and μ=20% showed a spike in the resistance for shallow penetration depth ($D/B \approx 0.025$), but follow close to the lower limit for the rest of the penetration. The spike in resistance may be because the shear bands have yet to be established for the shallow penetration.

The depth of initiated backflow is similar for all the models, except for the upper bound solution. The depth is between D/B=1.1 and D/B=1.21 for the softened soil and lower bound solution, while it is between D/B=1.37 and D/B=1.47 for the upper bound solution. The depth of initiated backflow is a bit inaccurately determined because the output frames of the deformation are a bit too scarce.

Strain-softening may increase the punch-through danger. As seen for the calculation with μ=20%, the punch-through danger is greater than for the lower bound solution. Strain-softening is therefore an important parameter in the material model. However, these calculations are hard to interpret because of the dependency of the element size regarding the shear band thickness. It would be interesting to know how large μ (absolute plastic strain for the softened condition) is needed to increase the punch-through potential drastically. It seems to be between 10-20% for this analysis, but it is not possible to conclude this, as a different mesh would probably give a different result. But Tjahyono's result showed a similar result, and it was concluded that μ < 5% could be calculated using the lower bound solution (no strain-softening), while this is not possible for μ > 5%.

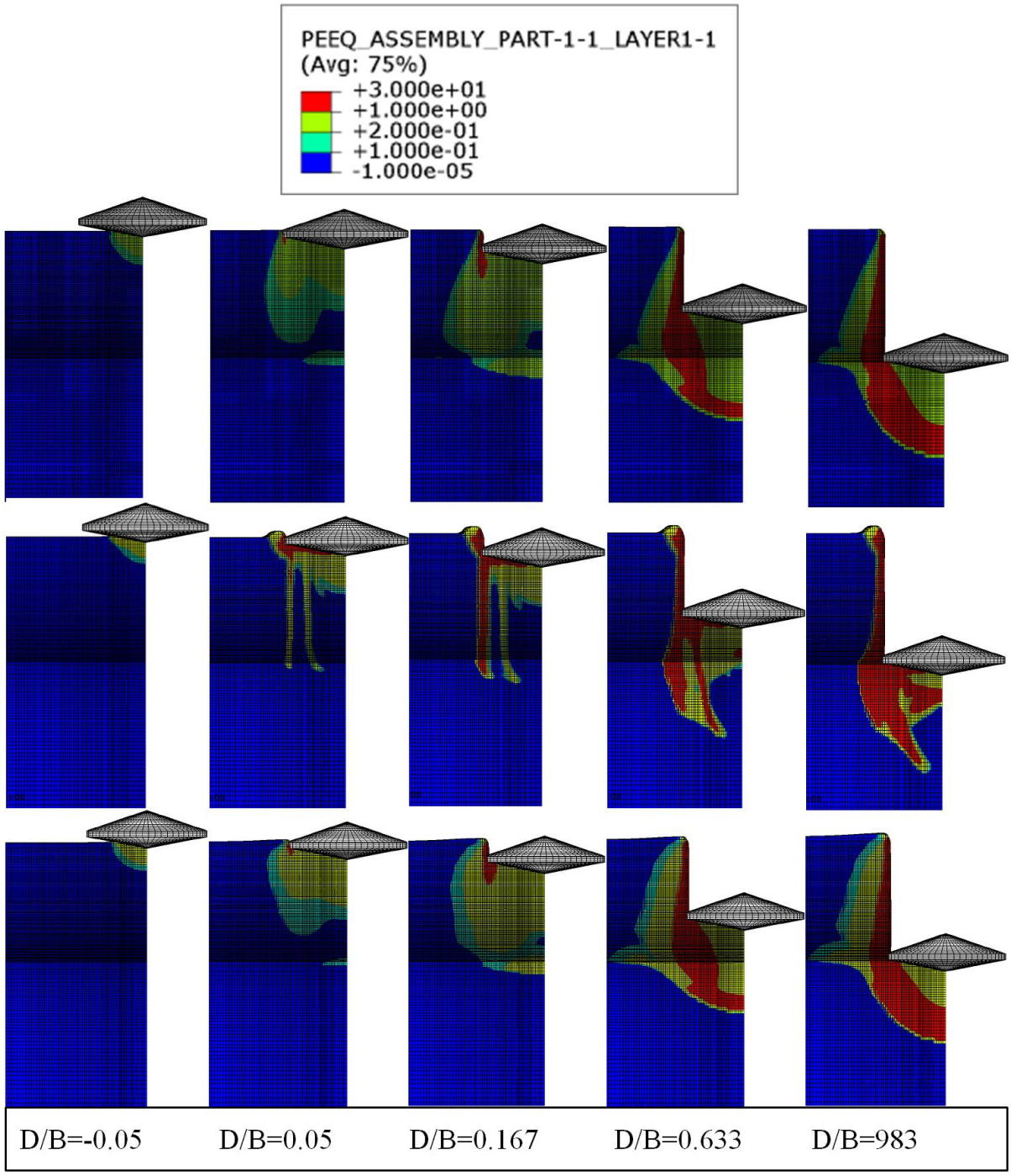

Figure 5-12 Countour plot of the absolute plastic strain in the upper layer. Pictures from the top: upper limit case, μ=20%, lower limit case.

5.2 H/B=0.5

5.2.1 Upper limit case

The calculations with H/B=0.5 were executed in the same manner as H/B=1. The upper layer still has a denser mesh compared to the lower layer, and the penetration speed is 1m/s. The model contains approximately 208.000 elements. The critical time step is 5.05E-5 seconds, and it took nearly 30 hours to complete the calculation.

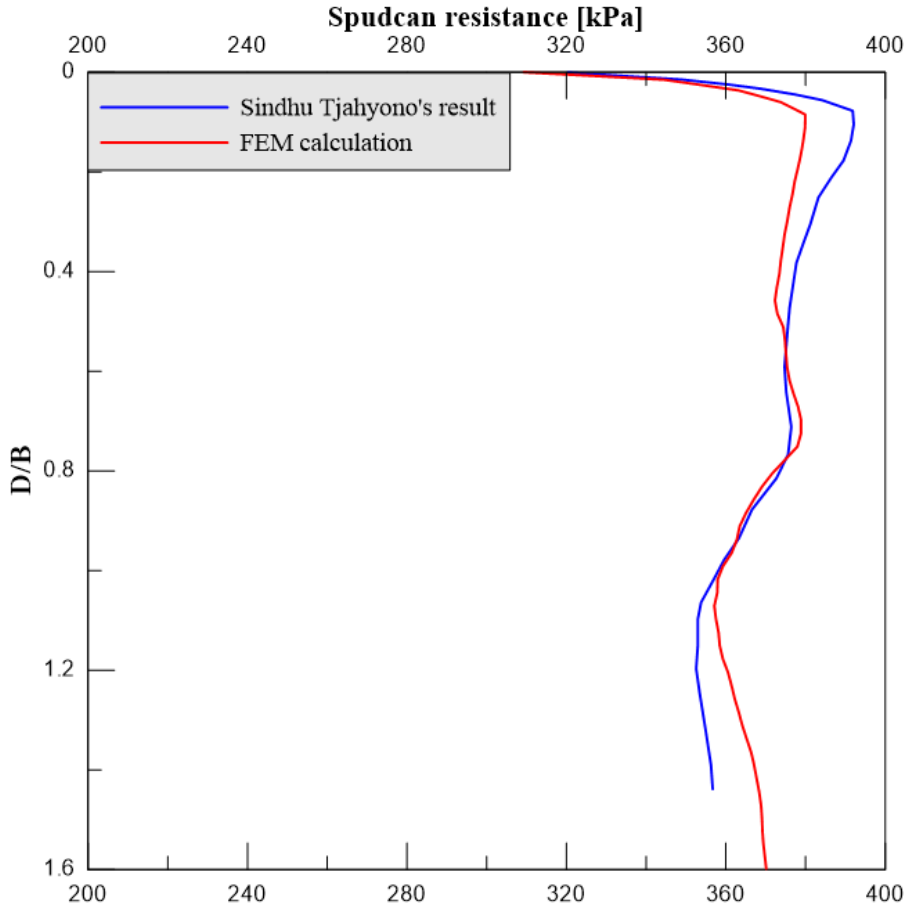

Figure 5-13 Spudcan resistance compared with Tjahyono's resut. H/B=0.5, c_{u1}=100kPa.

The spudcan resistance from the FEM calculation is plotted in Figure 5-13 together with Tjahyono's result from the same test. The results are similar to the calculation with H/B=1, where the resistance is a bit underestimated at shallow depths and overestimated in the lower layer. It is suspected that this is a direct result of different mesh resolution, where the element size is smaller in the top layer and larger in the bottom layer. The backflow is initiated around D/B=0.81, which is also the limiting cavity depth.

The spudcan resistance was also compared with the theoretical solution. The results are displayed in Figure 5-14. It is again evident that SNAME is an overly conservative estimate, as it underestimates the resistance and greatly overestimates the potential for punch-through. Hossain & Randolph's method perform better, but it also seems to underestimate the resistance. The depth of initiated backflow is calculated to D/B=0.97, which is a bit higher than the FEM calculation ($D/B \approx 0.81$). Tjahyono's hand calculation seems to perform much better, as we know that the resistance from the FEM calculation is possible underestimated at the top and overestimated at bottom. The depth of initiated backflow was calculated to D/B=0.82, which coincided very well with the FEM calculation (D/B=0.81).

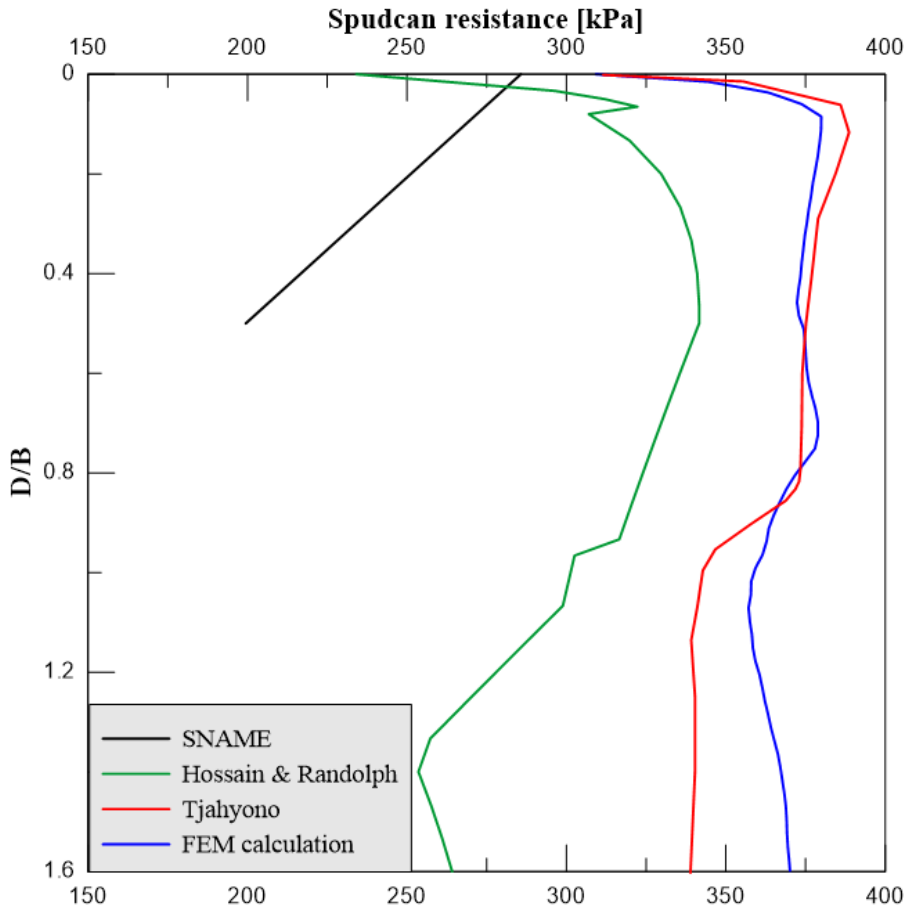

Figure 5-14 Spudcan resistance compared with hand calculations. H/B=0.5, c_{u1}=100kPa

5.2.2 Lower limit case

The lower limit case with pre-softened soil (c_{u1}=50kPa) was then calculated. The result is displayed in Figure 5-15. Again is the resistance underestimated in the top and overestimated in the bottom. This strengthens the suspected effect of the different element size. Smaller element sizes tends to reduce the resistance, as the shear bands will be established faster, and more localized strain will govern the deformation. In contrary, the larger elements increase the resistance because of broader shear bands which result in less localized strains. However, the localized strain and deformation in the shear bands are a realistic description of the deformation mechanisms, as it also occurs in a real test. But the thickness of the shear bands may be different, as it is only governed by the element sizes in the FEM calculations. The backflow is initiated around D/B=0.75 for this FEM calculation.

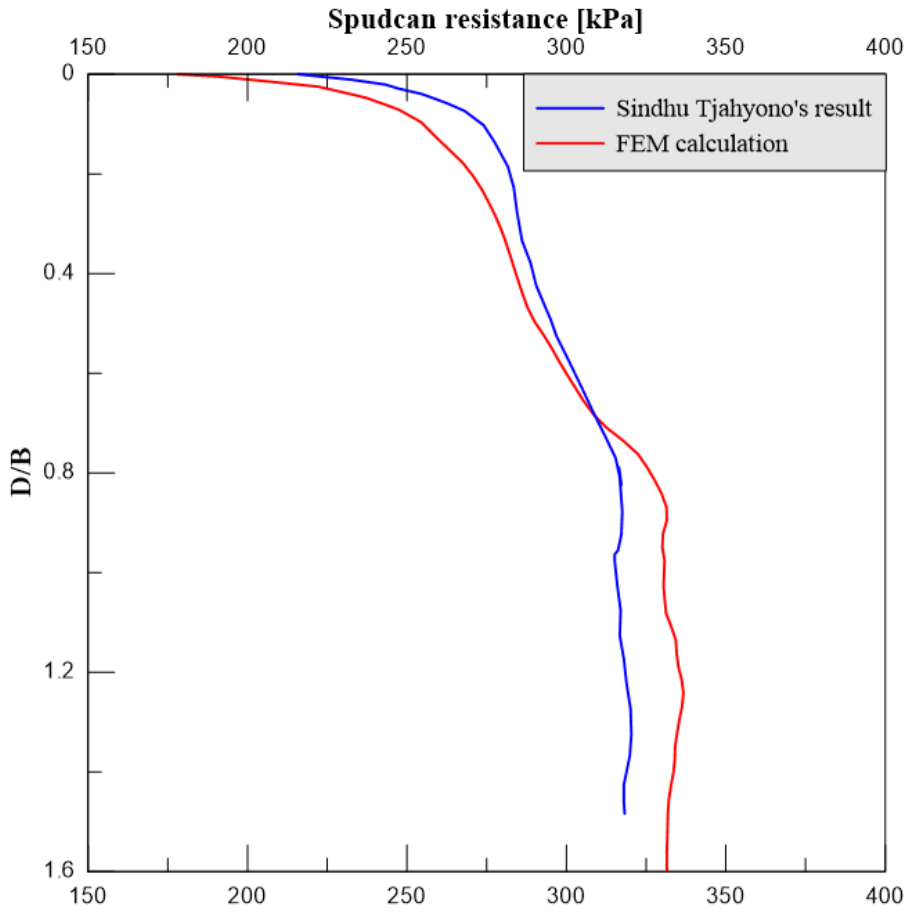

Figure 5-15 Spudcan resistance compared with Tjahyono's result. c_{u1}=50kPa and H/B=0.5

The FEM calculation compared to the theoretical solutions is plotted in Figure 5-16. SNAME preformed a bit better in this case compared to the upper limit case, but it is still underestimating the resistance. It does not really tell much of the expected mechanisms that are likely to happen, as it is only valid for the upper layer. Hossain & Randolph's method also performed better for this case. It does not underestimate the resistance as much, and the calculation in the upper layer seems to be very good. However, the reduction in resistance in the lower layer is seemingly too large compared to the FEM calculation. Back-flow is initiated at D/B=0.68 which is fairly close to the FEM model. At approximately D/B=1 is the resistance only govern by lower layer solution. Tjahyono's theoretical solution followed the FEM calculation in the same manner as Tjahyono's FEM calculation did, with a somewhat higher resistance in the upper layer, and lower resistance in the bottom layer. The depth of initiated backflow was calculated to D/B=0.74, which is very close to the FEM calculation ($D/B \approx 0.75$).

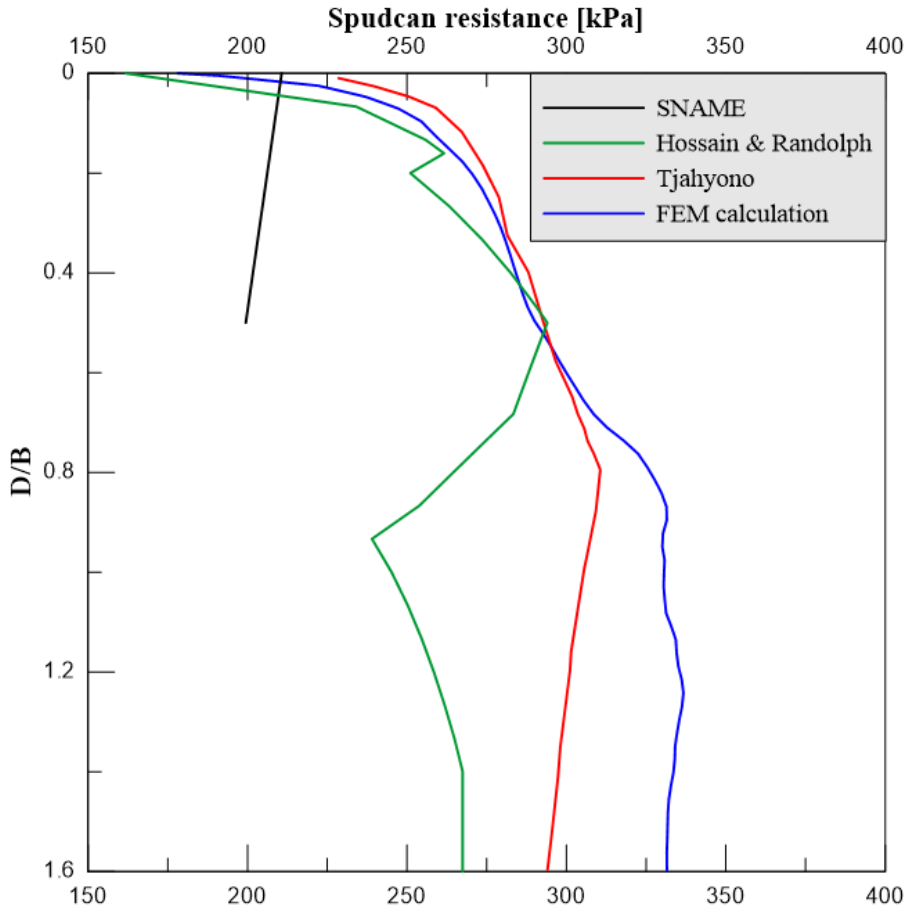

Figure 5-16 Spudcan resistance compared with hand calculations. H/B=0.5, c_{u1}=59kPa

5.2.3 Strain-Softening

Strain-softening was then introduced to the model in the same way as for H/B=1. The results are plotted in Figure 5-17. The model with μ=2% was not calculated because the difference between the lower limit case and μ=5% were virtually zero. As seen from the result, all the calculations are very close to the lower limit case. Only μ=20% show a small spike for shallow penetration. However, this was expected after the calculations with H/B=1, because reducing H/B would naturally reduce the penetration depth for which the shear bands were established. Tjahyono probably got larger differences in the result because the element size was larger in the top layer. But it was also concluded in Tjahyono's report that a reduced H/B would reduce the impact from μ (absolute plastic strain for which the soil is softened). H/B=0.5 would therefore be less affected by μ compared to H/B=1. This result shows again that interpreting the result with strain-softening have to be done with caution, as the strain-softening behavior is affected by the element size. It is therefore hard to conclude whether or not strain-softening behavior in the soil will increase the punch-through danger considerable. It does not seem to increase the punch-through danger from these FEM calculations, but Tjahyono got considerable larger affect from the strain-softening.

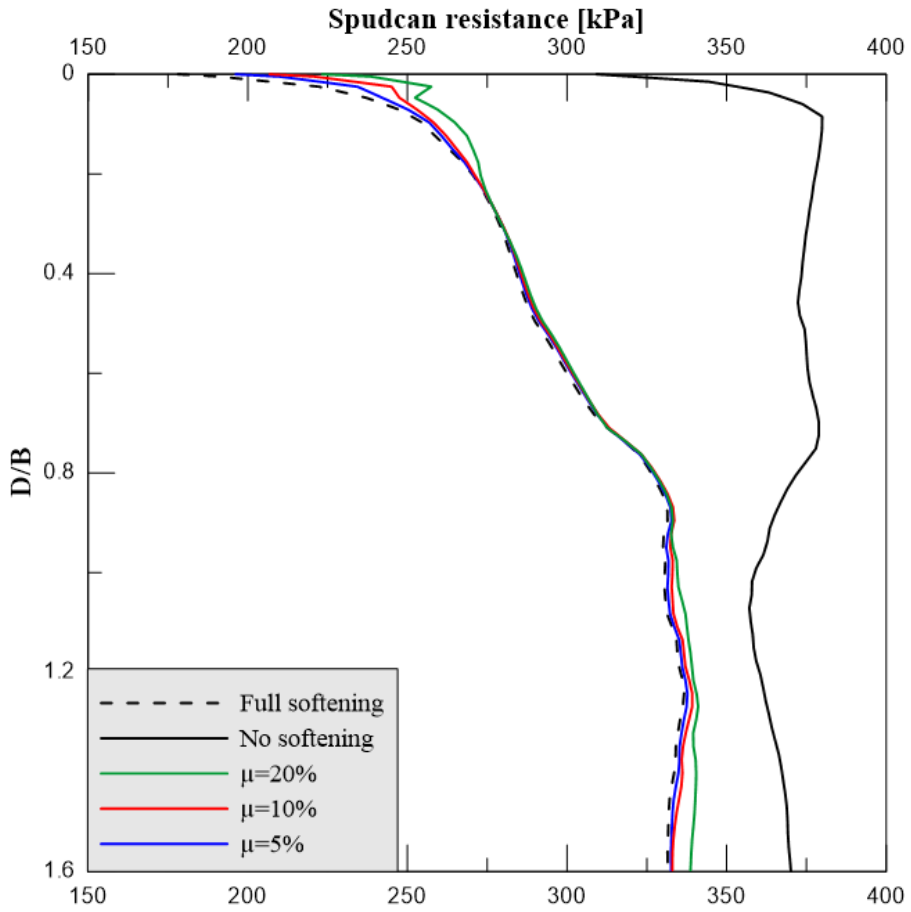

Figure 5-17 Spudcan resistance with strain-softening soil behaviour. H/B=0.5

5.3 Summary of spudcan penetration in two-layered clay

The main objective was to reconstruct Tjahyono's numerical experiment for two-layered clay, with and without strain-softening. The cases without stain-softening were also subject to comparison with the theoretical solutions, namely SNAME, Hossain & Randolph's and Tjahyono's method.

The comparisons with Tjahyono's FEM calculations revealed some effects from the element sizes in the eulerian mesh. Smaller elements were used in the top layer, and larger elements in the bottom layer. The smaller elements tend to reduce the spudcan resistance, while the larger elements increase the resistance. From the T-bar test is it evident that larger elements increase the amount of soil that flow around the structure, and consequently increasing the resistance. This explains why the larger elements in the lower layer increased the resistance as backflow was initiated. In addition, the resistance in the upper layer was reduced even though backflow was not initiated. This is likely to be because the shear bands will be established faster in denser mesh. The shear bands will also be more narrow and distinct for smaller elements, which lead to more localized strains in these zones.

The theoretical solutions varied a lot in performance. The SNAME method was an overly conservative estimate, as it underestimated the resistance and overestimated the punch-through danger. This is due to its whished-in-place approach where the deformed geometry is not accounted for. Some of the stronger upper layer will be pushed into the weaker lower layer, and this will increase the resistance and reduce the punch-through danger. Hossain & Randolph's method preformed much better as it is based on curve fitting from experimental data. However, it did underestimate the resistance compared to Tjahyono's method. Tjahyono's method seemed to work very well, except for the cases that H/B=1, where it was somewhat problematic to calculate the depth of initiated back-flow. As $\frac{H}{B} \geq \left(\frac{c_{u1}}{\gamma_1' B}\right)^{0.55}$ indicated that the backflow depth was within the upper layer, but it was clear from the FEM calculation that the backflow initiated in the lower layer (D/B≈1.4 as c_{u1}=100kPa). Except from this problem, Tjahyono's method was very accurate compared to the FEM calculation.

Strain-softening behavior in the upper layer was also analyzed. The sensitivity of the soil was set to 2, and the amount of absolute plastic strain needed to reach the softened state was varied from 2%-20% (μ). It was evident that the difference in spudcan resistance between the softening calculations was much smaller for this analysis (Figure 5-11, Figure 5-17) compared to Tjahyono's results (Figure 5-1). All the calculations were pretty similar to the lower bound solution. I suspect that the reason for this is that these models have smaller elements in the top layer compared to Tjahyono's model. The shear band thickness will therefore be narrower, and as a result, less resistance is measured. It also seems like the shear bands are established faster for denser mesh resolution. The strain-softening behavior has less effect when the shear bands are established. This is due to that the strains in the shear bands are much greater than the absolute plastic strain for which the soil is softened (μ). And the effect from μ is clearly smaller compared to Tjahyono's result. Reducing the thickness of the upper layer contributed

to this effect, as the shear bands were established even faster. Strain-softening soil behavior is therefore difficult to calculate and interpret. Increasing μ will lead to larger resistance and punch-through danger, but the effect of μ is also affected by the mesh resolution. Interpreting FEM calculations which include strain-softening should therefore be done carefully. It is possible to control the thickness of the shear bands with regularization methods such as non-local strain, but that was beyond the scope of this study.

Chapter 6. Summary & Conclusion

The preliminary tests revealed some of the challenges using the CEL method in Abaqus/Explicit. The triaxial compression test showed that the Young's modulus was correctly applied. The cohesive yield strength was a bit underestimated, but the error was low if sufficient mesh resolution was used. The element size and compression speed both affected the failure mode of soil sample. Reduced element size improved the numerical stability, while the compression speed mostly affected the failure mode and consequently changing the resistance after yielding was established. The speed also needed to be low enough to keep the dynamic energy low, as the test is in reality quasi-static. Triaxial compression with strain-softening soil behavior was harder to interpret. Mainly because the local strain-softening behavior in the shear bands will govern the resistance in the plastic part of the solution, and there are many solutions as a result of different failure modes. The width of the shear bands is also determined by the element size, which will affect the resistance. Smaller elements will give thinner shear bands, and consequently more localized strain-softening that will reduce the resistance. The interpretation of the results must therefore be done carefully.

The oedometer test showed that calculating large compressions with the CEL method in Abaqus/Explicit can be problematic. However, the solutions were stable up to a certain point of compression. This point was mainly determined by the element size, where smaller element increased the amount of compression that was possible before significant numerical instability occurred. The accuracy of problems involving very large compression forces is therefore constrained by computational power and time. The compression speed affected the amount of oscillations that occurred in the test result. However, these oscillations are possible to filter out if they oscillate around the right mean value. Finding the upper speed limit for which it is possible to filter out the oscillations may therefore reduce the calculation cost greatly.

The T-bar test was executed in order to study how the solution was affected by the element density and the penetration velocity. The theoretical value for the T-bar factor was not found, but an error less than 5% was obtained for the densest mesh resolution. Reducing the element size led to a smaller resistance, and the solution seemed to converge to the theoretical value. The reason why smaller element reduced the resistance is that less soil flowed around the T-bar, and the shear bands become more distinct and narrower. The speed did not seem to affect the overall resistance, but too high speed led to significant oscillations in the resistance. The correct resistance could be obtained by smoothing the resistance function, e.g. by taking the average value over a span of the penetration distance. However, this method can be a bit problematic if the rate of change of the resistance is too large, (e.g. start of the penetration). Calculations with strain-softening soil behavior were also conducted. Apparently, reasonable results were obtained, but the T-bar factor got reduced less than the cohesive yield strength. This is believed to be because nearly all the strain-softening occurred in the shear bands that were established. The resistance is therefore very much dependent on the element size, as smaller elements produce narrower shear bands and therefore less penetration resistance. The interpretation of the results containing strain-softening soil behavior must therefore be done

carefully. These tests showed again that the accuracy while using the CEL method in Abaqus/Explicit is constrained by computational power and time. It is, however, possible to get close to the theoretical solution for the T-bar test.

The spudcan penetration tests were initiated by checking the performance for penetration in homogenous one-layered clay. The bearing capacity were calculated from the resistance and compared to Marin & Randolph's upper and lower bound solution. The result was in reasonable agreement with Martin & Randolph's bearing capacity theory, except for shallow penetration, where the bearing capacity factor became too large. This was possible due to dynamic inertia effects from the first impact between the spudcan and the soil. However, the smoothing of the penetration resistance seemed to work well when the penetration rate was 1m/s. The result was otherwise within the upper and lower bound solution to Martin & Randolph, so the model seemed to perform with reasonable accuracy. The FEM calculation was numerical stable for the whole analysis, as the artificial energy was at maximum 2.43% of the internal energy (end of the penetration), and the kinetic energy was only significant for very shallow penetration ($D/B<0.01$).

Two cases with two-layered clay were calculated. The cases were found in Sindhu Tjahyono's doctor thesis "Experimental and numerical modelling of spudcan penetration in stiff clay overlying soft clay". One with $H/B=1$ and another with $H/B=0.5$, and each case had two limit calculations, where the cohesive yield strength in the upper layer was either non-softened (100kPa) or pre-softened (50kPa). The other calculations included strain-softening soil behaviour in the upper layer. The sensitivity was 2, and the absolute plastic strain for which the soil was softened (μ) was varied from 2% to 20%. The limit cases were subject to comparison with the theoretical solutions, while the strain-softening were only compared to Tjahyono's similar FEM calculations.

Comparison between the FEM calculations in this study and Tjahyono's study clarified some of the effects from the element size. Smaller elements reduce the resistance, while larger elements increase the resistance, which was also indicated by the preliminary tests. By comparing the strain-softening calculations in this study with Tjahyonos's result, it was evident that the affect from the parameter μ was a lot smaller. Nearly all the calculations were similar to the lower bound solution after only shallow penetration depth. This is probably because the shear bands had been established through the top layer to the lower layer earlier (for shallower penetration), and the strains in the shear bands are much larger than the parameter μ. Smaller elements would also give less resistance because the shear bands become narrower, and consequently more localized strain-softening will occur. This is important to know when calculation spudcan penetration in soil with strain-softening, because non-conservative result regarding the punch-through danger may be obtained if the elements are too small, as higher μ increased the resistance and punch-through danger. Interpreting FEM calculations which include strain-softening should therefore be done carefully.

Comparison between the FEM calculations and the theoretical solutions revealed some of the strengths and drawbacks with the theoretical solutions. SNAME preformed as expected, by overestimating the potential for punch-through and underestimating the spudcan resistance. It was most evident for the upper limit cases, as the reduction in the cohesive yield strength from the upper to the lower layer was largest. Hossain & Randolph's method performed in general well and the depth of initiated back-flow were close to the FEM calculations for most of the cases. But it also seemed to underestimate the resistance a bit if we compare to the FEM calculation from this study and Tjahyono's FEM calculation. Tjahyono's theoretical solutions worked in general very well. Yet, it was somewhat problematic to calculate the backflow depth for the case were H/B=1, as $\frac{H}{B} \geq \left(\frac{c_{u1}}{\gamma_1' B}\right)^{0.55}$ indicated that the backflow depth was within the upper layer, but it was clear from the FEM calculation that the backflow initiated in the lower layer (D/B≈1.4 as c_{u1}=100kPa). Except from this problem, Tjahyono's method proved to be very accurate compared to the FEM calculations in this study and Tjahyono's FEM calculations.

The coupled lagrangian-eulerian (CEL) method in Abaqus/Explicit has proven to be suitable for spudcan penetration problems, and the FEM calculations seemed to describe the soil mechanisms relatively accurate. However, there are some difficulties regarding the effects from the element size, especially when trying to include strain-softening behavior. It is important to address this problem, as non-conservative results might be obtained. The penetration speed affected mainly how much oscillation that occurs in the penetration resistance. The oscillation may be filtered out as the resistance oscillated around a mean value. The computational cost for these types of problems are large, and it is therefore of interest to find the highest penetration rate for which oscillations may be filtered out. Further studies should include regularization methods such as non-local strain in order to control the thickness of the shear bands.

References

Abaqus 6.12 Analysis User's Manual. (n.d.). *Eulerian Analysis, Chapter 14.1*.

Abaqus 6.12 Theory Manual. (n.d.). *Explicit dynamic analysis, Chapter 2.4.5.*

Abaqus/CAE User's manual. (n.d.). *Mohr-Coulomb plasticity, Chapter 23.3.3*.

Abaqus/CAE User's Manual. (n.d.). *The volume fraction tool, Chapter 28.5*.

Cook, R.D. & Malkus, D.S. & Plesha, M.E. & Witt, R.J. (2002). *Concepts and applications of finite element analysis* (Fourth Edition ed.). John Wiley & Sons, Inc.

Hossain, M. S. & Randolph, M. F. (2010). Deep-penetrating spudcan foundations on layered clays: numerical analysis. *Geotechnique, 60*(3), 171-184.

Hossain, M. S. (2008). *New mechanism-based design approaches for spudcan foundations in clay / Muhammad Shazzad Hossain.* PhD Thesis, University of Western Australia, Center of Offshore Foundation Systems.

Hossain, M.S. & Randolph, M.F. (2009, September). New Mechanism-Based Design Approach for Spudcan Foundations on Single Layer clay. *Journal of Geotechnical and Geoenvironmental Engineering, Vol. 135*(No. 9), 1264-1274.

Hossain, M.S. & Randolph, M.F. (2009). New mechanism-based design approach for spudcan foundations on stiff-over-soft clay. *Offshore Technology Conference.* Houston.

Liyanapathirana, D. M. (2008). Numerical simulation of T-bar penetration in soft clay. *GeoCongress*.

Martin, C.M. and Randolph, M.F. (2001). Application of the lower and upper bound theorems of plasticity to collapse of circular foundations. *Proc. 10th Int. Conf. of IACMAG*, *Vol 2.*, pp. 1417-1428. Tucson.

Nonlinear finite elements/Lagrangian and Eulerian descriptions. (2010, September 2). Retrieved April 23, 2013, from Wikiversity: http://en.wikiversity.org/wiki/Nonlinear_finite_elements/Lagrangian_and_Eulerian_descriptions

Nordal, S. (2012). *TBA4116 Geotechnical Engineering Advanced course Lecture notes and background material.* Trondheim: Tapir Akademisk Forlag.

Randolph, M.F. & Andersen, K.H. (2006). Numerical analysis of T-bar penetration in soft clay. *International journal of geomechanics*(6), 411-420.

Randolph, M.F. & Houlsby, G.T. (1984). The limiting pressure on a circular pile loaded laterally in cohesive soil. *Geotechnique, 34*(4), 613-623.

Stewart, D.P. & Randolph, M.F. (1994). T-bar penetration testing in soft clay. *Journal of Geotechnical Engineering*(12), 2230-2235.

Tjahyono, S. (2011). *Experimental and numerical modelling of spudcan penetration in stiff clay overlying soft clay.* PhD Thesis, National university of Singapore, Department of civil engineering, Singapore.

World Fleet of Jack-Up Drilling Rigs. (2012, October 10). Retrieved June 3, 2013, from http://shipbuildinghistory.com/today/highvalueships/offshorejackups.htm

Appendix A Speed converge T-bar test

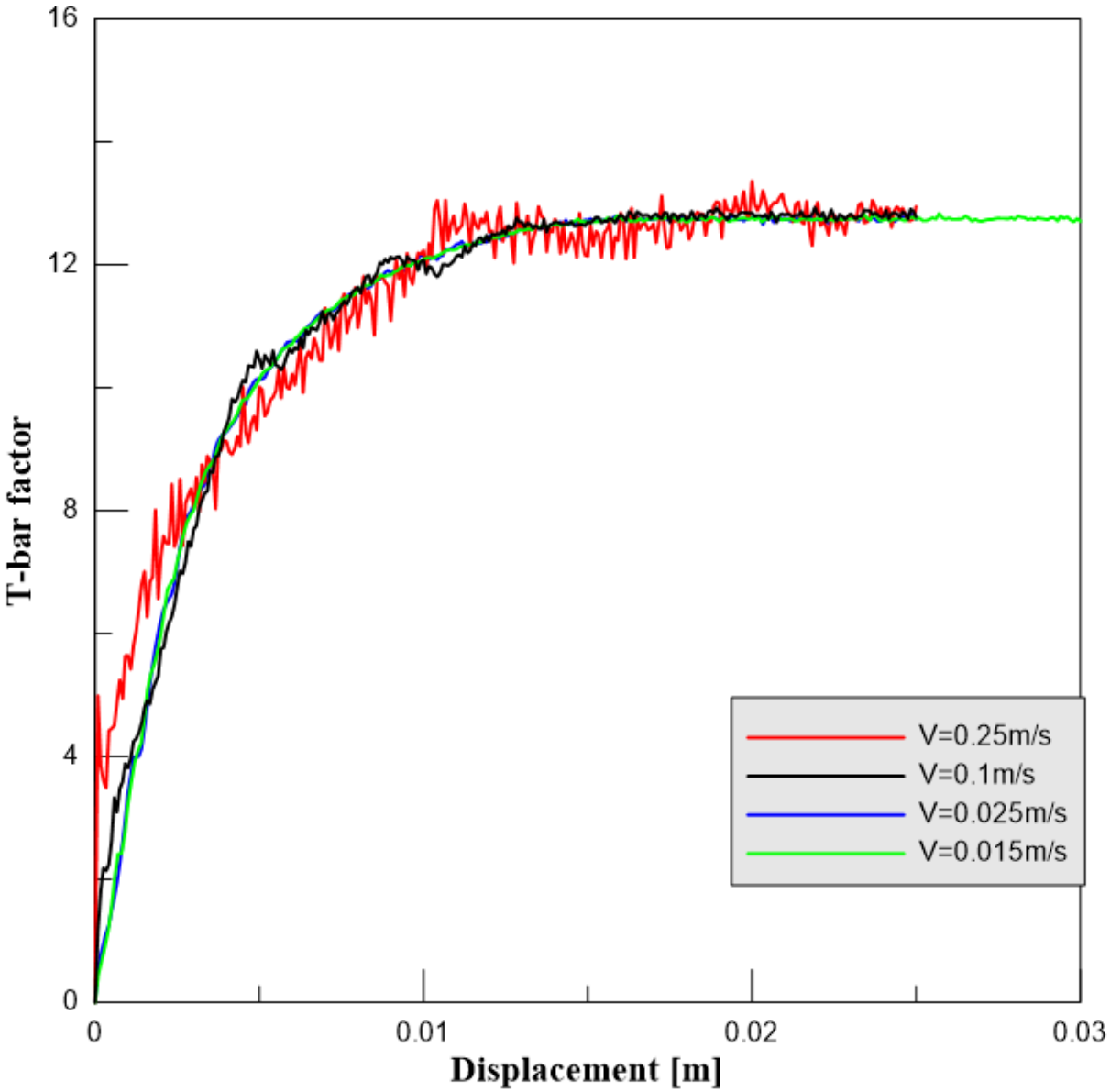

Figure A1 Speed convergence for T-bar test

Appendix B Spudcan penetration one layered clay

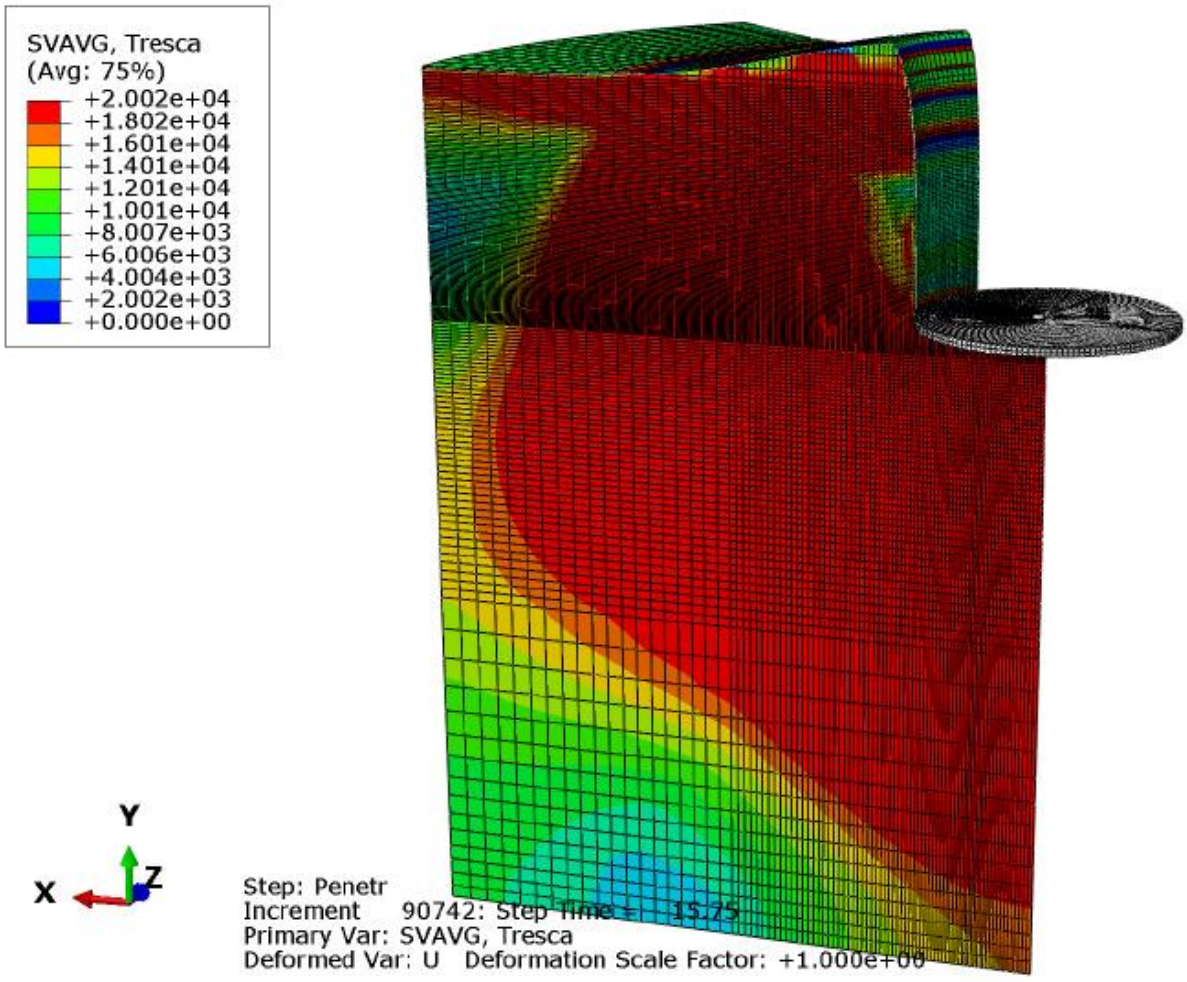

Figure B1 Contour plot of Tresca stress for one layered clay, as D/B=0.75

Appendix C Spudcan penetration two layered clay

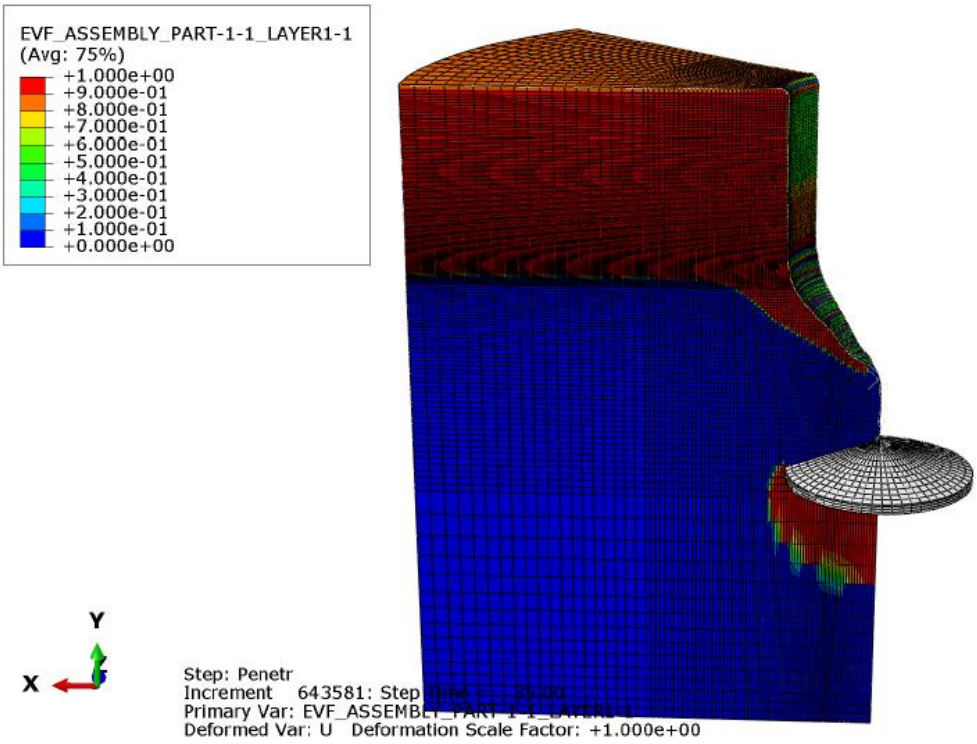

Figure C1 Contour plot of the upper layer at end of penetration for H/B=1, upper limith case.

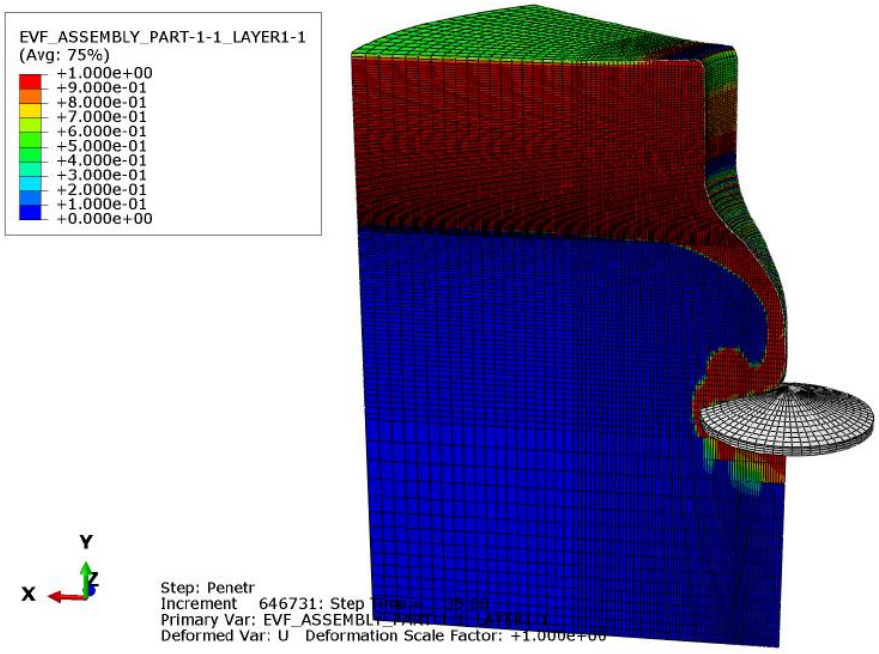

Figure C2 Contour plot of the upper layer at end of penetration for H/B=1, lower limit case.

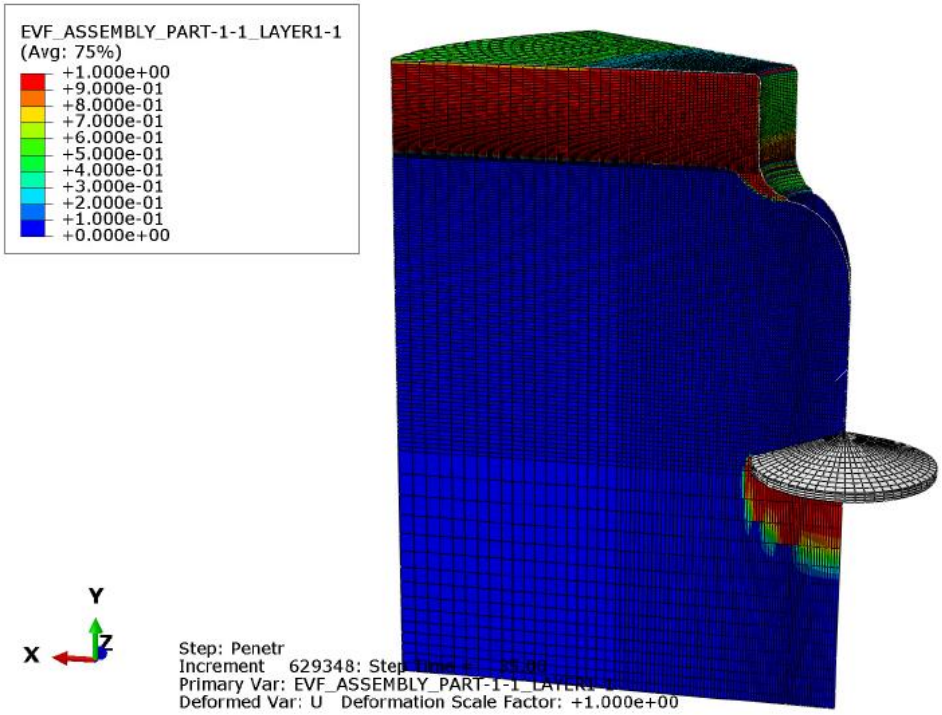

Figure C3 Contour plot of the upper layer at end of penetration for H/B=0.5, upper limit case.

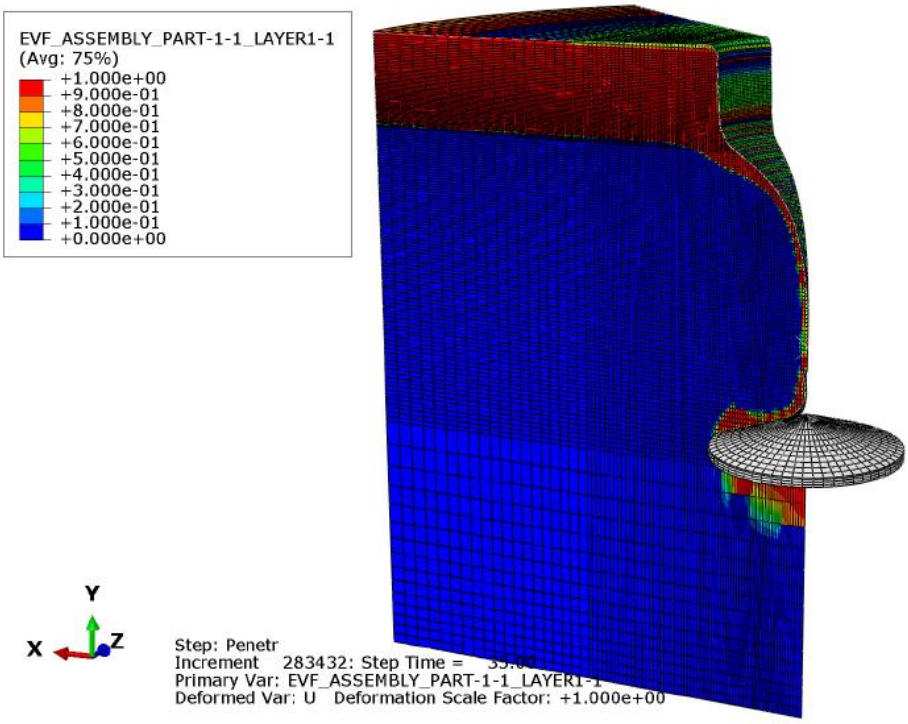

Figure C4 Contour plot of the upper layer at end of penetration for H/B=0.5, lower limit case.